

Long-range pair correlation and its role in small-angle scattering from fractal clusters

Anthony Pearson and Roger W. Anderson

Chemistry Department, University of California, Santa Cruz, California 95064

(Received 9 October 1992; revised manuscript received 14 May 1993)

The short- and long-range structures of computer-grown random-mass fractal clusters are described using exponential, Gaussian, and two different power-law pair-correlation functions. For all of the correlation functions the short-range structure is determined by the fractal dimension D and the long-range structure is expressed with a size parameter. One power correlation function has an additional shape parameter. Closed-form expressions are derived for the small-angle x-ray scattering for each of the four correlation functions. Clusters are grown using diffusion-limited-aggregation, Eden, dielectric-breakdown (DBM), ballistic, and random-polymer models. The Debye sum is used to calculate the small-angle scattering for each cluster. The parameters in the correlation functions are adjusted to provide the best fit to the Debye-sum scattering. The power laws reproduce the short- and long-range structural information much more accurately than the exponential or Gaussian models, which lack definitive size cutoffs and fractal scaling at intermediate- and long-range distances. In many cases the two-parameter power function produces fits that are as good as those with a third parameter. This indicates that the long-range shape parameter in the three-parameter power correlation function is simply related to the fractal dimension. The power fits accurately give the fractal dimensions and the radii of gyration for the clusters. Expressions are derived for the Guinier and the fractal-region scattering for each correlation function. Asymptotic formulas are used to explain large- q (fractal-region) scattering intensity that varies as $q^{-\nu}$, where $1 < \nu \leq 4$. It is shown for $D = 2$ systems that the fractal scattering is independent of the size and shape parameters. The extensions of this work to the scattering by multifractals are discussed. An efficient method is also presented to calculate large DBM clusters with noninteger growth exponents.

I. INTRODUCTION

This paper presents results on the determination of general structural information about clusters and other large molecular objects. The traditional goal in structure work is the determination of the precise position of each particle in the cluster. This can be accomplished with direct imaging of the object or with extensive x-ray-scattering measurements if the substance can be crystallized. The result is a large table of coordinates that defines the structure. However, it is not always possible to obtain crystals of a substance, and for other cases random variations in the structure prohibit precise structure determination. For these cases simple, cruder measures of structure are useful, and such measures can also provide a simple summary of a detailed molecular structure.

Here we consider the structural information in the pair-correlation function $p(r)$ that gives the number of pairs of particles, $p(r)dr$, in the cluster with distances between, r and $r + dr$. We seek to understand these correlations at both short- and long-range distances. If the cluster is assumed to be a *simple mass fractal*, then we can write

$$p(r) = r^{D-1}f(r). \quad (1)$$

where D is the fractal dimension and $f(r)$ is a cutoff function that assures a finite number of particles (size) for the cluster. The cutoff function is assumed to be nonzero and finite at $r = 0$. At short range the pair-correlation

functions $p(r)$ scale as r^{D-1} , and the number of particles found within a distance r is proportional to r^D . Alternatively the short-range scaling can be expressed with the density-density correlation function $c(r)$, which can be expressed as r^{D-d} , as characterized by many workers (Refs. 1 [p. 339, Eq. (1.2)], 2, and 3). Here d is the dimension of Euclidean space in which the cluster resides. However, the radius of gyration, R_g , and the maximum pair distance, the *spanning length* a , are determined by both D and $f(r)$. The pair-correlation function expressed as Eq. (1) is exact for solid spheres, where the cutoff function $f(r)$ is proportional to the characteristic function $\gamma_0(r)$ which was introduced by Porod (Ref. 4 p. 12). However, the form of $p(r)$ expressed in Eq. (1) is phenomenological for fractal clusters, and to date we know of no fundamental theory that even gives the form of $f(r)$ for fractal clusters.

If the coordinates of all particles in a cluster are known, then $p(r)$ is easily calculated and a fractal dimension D and a cutoff function $f(r)$ can be fit to the actual $p(r)$. This will explicitly determine D and $f(r)$. Quantities such as R_g and a can be easily determined. But for many physical clusters, detailed coordinate data will not be known, and small-angle scattering experiments may be used to determine D and $f(r)$. The theory of scattering from fractal objects was addressed as early 1983 by Witten and Sander⁵ who correctly predicted the Fourier reciprocity relationship between real space and q space for fractal objects at large q . If $D < 3$, it can be shown⁶ that

the scattering intensity decreases as q^{-D} for the large- q region, if $f(r)$ approaches zero sufficiently quickly for large r . This q^{-D} dependence has been used extensively to elucidate the general and fractal structure of materials such as silica aerogels,⁷ resin polymers,⁸ proteins,⁹ and detergent-type structures.¹⁰ Other materials which have been investigated include bone, aerosols, soot, and smoke. In other work on glasses¹¹ and carbonaceous coal deposits¹² the scattering is observed to have an inverse power dependence on q , but the scattering is not discussed in terms of mass fractals. In the cases where the material is nonabsorbing and has a large enough particle size, light scattering instead of small-angle x-ray scattering (SAXS) or small-angle neutron scattering (SANS) has been used in the determination of fractal dimensions.

The main emphasis of this paper is an examination of $f(r)$, which we do by considering the small-angle scattering for different assumed forms for $f(r)$. Exponential, Gaussian, and power forms are used. The power forms for $f(r)$ are chosen to be zero for $r \geq a$. One of the power models contains an additional parameter μ that determines the form of $p(r)$ as $r \rightarrow a$. We find closed-form expressions for the small-angle scattering intensity $I(q)$ for each $f(r)$, where $I(q)$ will depend on the values of two or three parameters.

We attempt to find the best form for $f(r)$ by comparing the best fits that can be obtained with the scattering from the assumed $f(r)$ and the calculated synthetic scattering of computer-grown random clusters. The scattering has been determined for clusters ranging from 10^3 to 10^5 atoms, which we have grown with diffusion-limited-aggregation (DLA) [Refs. 13 (pp. 134–181), 3, 5, and 14], Eden,¹⁵ ballistic,¹⁶ and dielectric-breakdown [Refs. 17, 18, and 19 (p. 151)] (DBM) models. The DLA model uses a random-walk method to choose and follow the trajectories leading to growth. The DBM model solves the Laplace equation in two or three dimensions to generate the probabilities for the addition of particles according to the rules set forth by Niemeyer, Pietronero, and Wiesmann.¹⁷ The DBM model uses an adjustable parameter η that when increased from 0 to 1 produces structures with *variable* fractal dimensions D that decrease from 3 to $\simeq 2.5$.

We judge our choices for $p(r)$ on their ability to reproduce the known R_g , a , and D for the computer-generated clusters after adjusting the parameters in the $p(r)$ to provide the best fit to the synthetic scattering. An important aspect of this work is that we find properties such as D for fractal clusters from global fits of $I(q)$. Hence we demand a $p(r)$ that has information about all distances in the cluster. The $p(r)$ at small r is determined by D and at large r by the size of the cluster and the functional form of $p(r)$. In recent SAXS determinations of the fractal dimension of complex aggregate structures^{9,8,20} this global approach has been avoided. Typically workers examine $I(q)$ for simple q^{-D} behavior, or they use the intensity expression derived from an exponential cutoff function to fit the large- q scattering. We will show that these approaches can have significant errors for all of the properties of *monodisperse* fractal clusters. An important reason for the failure of simple models is that the scattering

for monodisperse clusters is often oscillatory. Polydispersity will smooth the oscillations, but the extent of the polydispersity is different for various real materials. The results of this paper can be extended to include any distribution of cluster sizes. However, since we are using the theory for the scattering by computer-generated clusters that have a unique size, we do not consider polydispersity here.

Our techniques can be applied to any monodisperse system of random clusters which are nonaggregating. Aggregation phenomena can be examined if the aggregation is based upon a monomeric unit for which the structure factor is known. The scatterers are assumed to take on all orientations and to be noninteracting with the other clusters in the sample (dilute assumption). The fractal dimension D will be most reliably determined if the cluster is a simple fractal (single value for D) and has approximate spherical symmetry.

Section II of this paper reviews small-angle scattering theory and the calculation of scattering with the Debye sum and its integral approximation. Section III introduces the four pair-correlation functions $p(r)$ that are used in this work. The corresponding expressions for $I(q)$ are presented along with the limiting forms for small and large q . It is shown that the large- q scattering intensity is independent of the form of $f(r)$ for $D = 2$ clusters. Section IV discusses the methods we use to generate the clusters for the synthetic-scattering data. An efficient algorithm is presented for the calculation of DBM clusters. Section V gives the results for the fits of the synthetic scattering with the four assumed correlation functions. The best-fit $p(r)$ are compared with the actual pair-correlation functions for the computer-grown clusters. Section VI discusses the strengths and weaknesses of the pair-correlation functional forms. The relationship of this work with surface and multifractals is considered.

II. SMALL-ANGLE X-RAY SCATTERING

In this section we consider x-ray scattering that is derived from the Debye sum. The theory can also be used to treat light scattering, neutron scattering, and electron diffraction. SAXS is calculated from the real-space coordinate data of each cluster with N particles using the Debye sum:

$$I(q) = \sum_{i,j=1}^N \frac{f_i(q)f_j(q) \sin(qr_{ij})}{qr_{ij}}. \quad (2)$$

In this equation $f_i(q)$ is the scattering factor for the i th particle in the cluster, and r_{ij} is the distance between particles i and j . The magnitude of the scattering vector q is given by $q = 4\pi \sin(\theta/2)/\lambda_0$, where θ is the scattering angle, and λ_0 is the wavelength of the scattered particle. This is the wavelength of a photon or the de Broglie wavelength of a neutron or an electron. In this work, the unit for λ_0 will be the unit distance r_0 on the lattice on which a cluster is grown. The unit for q is r_0^{-1} .

For a cubic lattice r_0 is also the minimum interatomic distance.

Here we will consider only clusters composed of a single type of particle. In this case the Debye sum can be written as

$$I(q) = P(q) \sum_{i,j=1}^N \frac{\sin(qr_{ij})}{qr_{ij}}, \quad (3)$$

where $P(q) = f^2(q)$ is the scattering for one particle. The scattering at zero θ or q is $I(0) = P(q)N^2$. In this paper we will assume that the particles are structureless point scatterers, so that $P(q)$ can be taken as unity with no q dependence. To calculate the scattering for clusters composed of particles with a $P(q)$ that varies in the q space of interest, scattering-intensity equations in this paper need only be multiplied by $P(q)$.

The Debye sum is an exact method for representing scattering from a cluster of ideal noninteracting point centers, where the cluster is randomly oriented in space. Using the Debye sum allows exact Fourier component summation, such that all the detail that is usually found in precise x-ray-diffraction experiments from very dilute homogeneous size samples is preserved.²¹ The extension of our results to polydisperse samples is beyond the scope of this work, and this theory only deals with monodisperse samples in the small-angle region where $q \leq 1$. It will be shown that different cluster-growth models lead to a variety of different behaviors in q space.

A general property of scattering for small q is that it is determined by the radius of gyration, R_g , for the cluster. In this work the unit of R_g is r_0 . The scattering for $q < 1/R_g$ is called Guinier scattering and is always given (Ref. 4, p. 27) as

$$I(q) \approx I(0)(1 - R_g^2 q^2/3 + \dots). \quad (4)$$

This result is the basis of the most commonly used method to determine particle size.

For most of the clusters that have been considered in this work, the particles occupy integer lattice points in two- or three-dimensional space. Hence the position of each particle is given by (i, j, k) where i is the x position, j is the y position, and k is the z position. For such lattices the Debye sum can be efficiently calculated. One might expect that the calculation would need N^2 trigonometric functions for a cluster with N particles. However, the cubic lattice implies that the squares of all distances r within the cluster are sums of three square integers: $r^2 = i^2 + j^2 + k^2$. The possible values for r^2 are 1,2,3,4,5,6,8,..., a^2 , where a is the largest distance (spanning length) in the cluster. Some of the square distances such as 7 are not possible because the number cannot be represented as the sum of three square integers. The number of possible distances $\sim a^2$ in the cluster is much smaller than N^2 , and so the best strategy to calculate $I(q)$ by the Debye sum is to first write the sum as

$$I(q) = P(q) \left(N + 2 \sum_{i=j+1}^N \sum_{j=1}^{N-1} \frac{\sin(qr_{ij})}{qr_{ij}} \right). \quad (5)$$

Now setting $x = r^2$ and $P(q) = 1$,

$$I(q) = N + \sum_{x=1}^{a^2} p_x \frac{\sin(qx^{1/2})}{qx^{1/2}}, \quad (6)$$

where p_x is the total number of pairs of particles that are separated by the distance $x^{1/2}$. This equation shows that it is best to first accumulate the number of particles separated at each of the possible distances and then evaluate less than a^2 trigonometric functions.

The Debye sum is useful to accurately calculate the scattering from clusters of known structure. However, it is not useful for prediction of special properties of the scattering from fractal clusters or for the extraction of the pair-correlation function from observed SAXS. For these purposes the summation can be approximated by an integral.

$$I(q) = N \int_0^\infty p(r) \frac{\sin(qr)}{qr} dr. \quad (7)$$

In this equation we will call $p(r)$ the pair-correlation function, and the average number of neighbors for an atom in the cluster at a distance between r and $r + dr$ is $p(r)dr$. We define $p(r)$ in this way because we will determine the parameters in $p(r)$ using only relative scattering intensities $I(q)/I(0)$. The normalization of $p(r)$ is

$$\int_0^\infty p(r) dr = N. \quad (8)$$

To complete the continuum formulation, we assume that $p(r)$ has the form $p(r) = r^{D-1}f(r)$, where $f(r)$ vanishes for large r to yield a cluster with N particles. D is a *mass-fractal* dimension and gives the number of particles within a distance r as $r^D f(0)/D$ for small r . If $D = 3$ and $f(0) = 4\pi$, the expected result for a sphere is found. In this case $f(r) = 4\pi\gamma_0(r)$, where $\gamma_0(r)$ is Porod's characteristic function. In this work we will consider four $f(r)$ functions that have closed-form expressions for $I(q)$.

It is important to consider the validity of Eq. (7) that approximates the Debye-sum expression for the scattering by an integral over the pair-correlation function. For a cluster that is grown on a lattice of unit length, the Debye sum gives scattering that is large for small q and that tends to decrease as q is increased. The scattering envelope will have a minimum value for $q < 2\pi$, where $q = 2\pi$ is the first Bragg diffraction. Since the scattering from our assumed $p(r)$ continues to decrease as q increases, we expect that Eq. (7) will fail for sufficiently large q . Here our task is to show that Eq. (7) is valid for $q \leq 1$, where the units of q have been defined earlier.

In the literature,²² the integral representation of $I(q)$ is often given as

$$I(q)/N = \int_0^\infty p(r) \frac{\sin(qr)}{qr} dr + C, \quad (9)$$

where the constant $C = 1/D$ is intended to correct the fact that the Debye-sum scattering envelope will have a minimum value. The added constant has also been

justified to account for self-scattering. However, we will now argue that it is justified to set $C = 0$ to describe the scattering for $q \leq 1$. This choice for C has been done by others^{23,24} without justification. Setting $C = 0$ allows us to use Eq. (7) or more specifically Eq. (14) in this work. One useful consequence of the following arguments is that they show that the small-angle scattering region extends at least to $q = 1$.

We can give three justifications for the neglect of C . The first can be seen in the following justification for the integral expression for $I(q)$ that is based on the Euler-Maclaurin sum formula [Ref. 25, p. 16, Eq. (3.6.28)]:

$$\sum_{k=1}^{n-1} f_k = \int_0^n f(k) dk - \frac{1}{2}[f(0) + f(n)] + \frac{1}{12}[f'(n) - f'(0)] + \dots \quad (10)$$

Although the series on the right-hand side of this equation may not be absolutely convergent for actual correlation functions, we assume as is done in perturbation theory that the first few terms will allow an estimate of the errors in the approximation of the sum by an integral. With this Eq. (6) can be rewritten as

$$I(q) \simeq N \left(\int_0^{a^2} p(x) \frac{\sin(qx^{1/2})}{qx^{1/2}} dx + 1 - \frac{1}{2} p_0 - \frac{d}{dx} \left[\frac{p(x) \sin qx^{1/2}}{12qx^{1/2}} \right]_{x=0} \right), \quad (11)$$

if a^2 is chosen large enough that $p(x) \sin(qx^{1/2})/(qx^{1/2})$ and its derivatives can be neglected at the upper limit of the summation. The task now becomes the estimation of the derivative term. This term can be expanded as

$$\frac{1}{12} \left[p'(0) + p_0 \frac{d}{dx} \left(\frac{\sin qx^{1/2}}{qx^{1/2}} \right)_{x=0} \right]. \quad (12)$$

We use a finite-difference approximation that $p'(0)$ is given by $p_1 - p_0$. A consistent choice for p_1 is $2D$, since this gives the correct number of nearest neighbors for $D = 1, 2, 3$. With $p_0 = 1$ the final expression for $I(q)$ is

$$I(q)/N \simeq \int_0^\infty p(r) \frac{\sin(qr)}{qr} dr + \frac{7-2D}{12} + \frac{q^2}{72}. \quad (13)$$

This argument shows that the end-point correction has a small q dependence, but the magnitude of the correction is only $1/12$ for $D = 3$ and $1/4$ for $D = 2$ provided that q is less than or equal to 1. Since the integral is N at $q \simeq 0$ and of order of 1 at $q = 1$, the correction can only affect $I(q)$ for q near 1, and then only by 1 part in 12 for most three-dimensional clusters. For lower-dimensional clusters $I(q)$ is greater than 1 for $q = 1$, and so the correction is still small. It appears justified to neglect an additional constant for a cluster containing thousands of atoms.

Now that we have begun the justification of the integral approximation to the Debye sum, we start using a simpler expression for the scattering intensity. We will write Eq. (7) without the factor of N as the following:

$$I(q) = \int_0^\infty p(r) \frac{\sin(qr)}{qr} dr. \quad (14)$$

This equation is sufficient to interpret all of the fits in this paper, because only the ratio of $I(q)/I(0)$ is considered. If absolute intensities are desired, careful evaluation of $P(q)$ must be done and the factor of N must be reinserted.

The second reason to omit an added constant is that the Debye scattering from all the lattice points within a spherical boundary is accurately reproduced by Eq. (14). In this case

$$p(r) = 4\pi r^2 (1 - r/a)^2 (1 + r/2a), \quad (15)$$

where a is the diameter of the sphere. Now Eq. (14) was evaluated by Rayleigh (Ref. 4, p. 19) to give

$$I(q) = \frac{9\pi}{2} \left(\frac{J_{3/2}(qa/2)}{(qa/2)^{3/2}} \right)^2. \quad (16)$$

The third reason to neglect the self-scattering term is that none of the $p(r)$ discussed in this paper fit the synthetic data well enough to include the term.

The fact that Eq. (16) accurately reproduces the Debye scattering for the set of all cubic lattice points enclosed by a sphere also indicates that the presence of the many zeros in the actual discrete correlation function does not significantly impair the continuum approximation. It appears that only the average of the discrete correlation over several zeros is important.

Several important properties of the scattering can be obtained from Eq. (14). If $D=3$ and $f'(0) < 0$, the scattering decreases as q^{-4} for $1/R_g \leq q \leq 1$. This is called Porod scattering. If $D < 3$, it can be shown⁶ that the scattering intensity decreases as q^{-D} in this q region, if $f(r)$ approaches zero sufficiently quickly for large r . We will call this *fractal scattering*.

In principle, the pair-correlation function can be obtained by direct inversion of the small-angle form of the scattering intensity by means of the equation

$$p(r) = \frac{2r}{\pi} \int_0^\infty q I(q) \sin(qr) dq. \quad (17)$$

However, this inverse transformation is difficult to do with experimental data. Experimental data has noise and is often convoluted with slit corrections and the like. Also the small-angle form of the $I(q)$ data must be extrapolated to large values of q to capture all contributions to the integral. The final problem with direct inversion is that the result will be $p(r)$ at a set of r values. Quantities such as the fractal dimension must then be estimated from these numerical $p(r)$ values. Our approach in this paper will be to fit actual $I(q)$ by varying parameters in assumed forms for the pair-correlation function. There is no experimental averaging of the data we will use, but this simulation procedure can easily be extended to experimental data that contains such averaging.

III. PAIR-CORRELATION FUNCTIONS AND THEIR SCATTERING INTENSITY

We now present four different continuous $p(r)$ distributions that will hopefully be good representations of the discontinuous pair-correlation functions found in real fractal clusters. These $p(r)$ are chosen to be physically reasonable and result in closed-form expressions for $I(q)$. The parameters in the assumed $p(r)$ will be adjusted to best-fit Debye scattering from computer-generated random clusters.

The first has an exponential $f(r)$, $p(r) = r^{D-1} \exp(-r/\lambda)$, which has often been used by other workers.^{10,24,26-28} The parameter λ is a measure of the size of the cluster. The second has a Gaussian $f(r)$, $p(r) = r^{D-1} \exp(-r^2/\xi^2)$. Here ξ is the size parameter. In this case the pair-correlation function decreases more quickly with r than for the exponential, but the $p(r)$ still extends to arbitrarily large r .

The other two choices for $p(r)$ are motivated by Eq. (15), which gives the pair-correlation function for a sphere. If the $1 + r/2a$ and 4π factors are suppressed, the sphere-correlation function has the form $p(r) = r^{D-1}(1 - a/r)^{D-1}$. Here the parameter a is the spanning length and the large r dependence of $p(r)$ is described by $D - 1$. We call this correlation function the modified power law or the two-parameter power law, and we use it as our third choice. The fourth correlation function is the three-parameter power law $p(r) = r^{D-1}(1 - r/a)^\mu$.

Here the parameter a is the spanning length and μ is a shape parameter describing the long-range dependence of the correlation function. The modified power correlation function is obtained from the power-law function by setting $\mu = D - 1$.

These correlation functions result in analytic functions for the scattered intensity. The well-known (Refs. 22 [p. 155, Eq. (36)], 24, and 29 [p. 72, Eq. (7)]) result for the exponential $f(r)$ is

$$I(q) = \frac{\lambda^{D-1} \Gamma(D-1)}{q(1 + q^2 \lambda^2)^{(D-1)/2}} \sin[(D-1) \tan^{-1}(\lambda q)]. \quad (18)$$

The computational simplicity of this equation accounts for its heavy use.

The scattering intensity for the Gaussian correlation function is given by (Refs. 30 [p. 495, Eq. (7)] and 29 [p. 74, Eq. (24)])

$$I(q) = \frac{\xi^D \Gamma(D/2)}{2} {}_1F_1\left(\frac{D}{2}; \frac{3}{2}; -\frac{\xi^2 q^2}{4}\right), \quad (19)$$

where ${}_1F_1$ is the well-known confluent hypergeometric function (Ref. 25, pp. 503-535).

The power-law function results in $I(q)$ given as a sum of two confluent hypergeometric functions of imaginary argument (Refs. 30 [p. 425, Eq. (11)] and 29 [p. 68, Eq. (5)]):

$$I(q) = \frac{a^{D-1} \Gamma(D-1) \Gamma(\mu+1)}{2iq \Gamma(\mu+D)} [{}_1F_1(D-1; \mu+D; iaq) - {}_1F_1(D-1; \mu+D; -iaq)]. \quad (20)$$

$I(q)$ for the modified power-law function can be found in terms of Bessel and Beta, $B(x, y)$, functions:

$$I(q) = \frac{a^{D-1} B(D, D-1) \Gamma(D - \frac{1}{2})}{q} \left(\frac{1}{4}aq\right)^{D-\frac{3}{2}} \left[\sin\left(\frac{1}{2}aq\right) J_{D-\frac{3}{2}}\left(\frac{1}{2}aq\right) - \cos\left(\frac{1}{2}aq\right) J_{D-\frac{1}{2}}\left(\frac{1}{2}aq\right) \right]. \quad (21)$$

The derivation of the above expression in terms of Bessel functions is accomplished by equating the series expansions for the confluent hypergeometric functions [Ref. 25, p. 504, Eq. (13.1.2)] with those for the Bessel functions [Ref. 25, p. 360, Eq. (9.1.10)].

The actual computations for the exponential are trivial, but the other correlation functions lead to the ${}_1F_1$ and noninteger-order Bessel-function expressions,^{25,30} which are more difficult to calculate. We have found that the algorithms of Luke³¹ provide a convenient way to accurately evaluate the ${}_1F_1$ (Ref. 31, pp. 20, 73-75, 93-96) and Bessel functions (Ref. 31, pp. 208-209).

We now summarize analytical results for Guinier and fractal scattering for each of the four correlation functions. Guinier scattering occurs for small q , where $I(q)$ can be expressed with the first terms of a series expansion about $q = 0$, as in Eq. (4). Only terms with even powers of q appear in the series expansion.

The exponential model has a small- q expansion given by

$$I(q) = \lambda^D \Gamma(D) \left(1 - \frac{D(D+1)\lambda^2 q^2}{6} + \dots\right). \quad (22)$$

Using Eq. (4) and the approximation from the exponential above, the radius of gyration is given by

$$R_g^2 = \frac{D(D+1)\lambda^2}{2}. \quad (23)$$

The Gaussian model has a small- q expansion given by

$$I(q) = \frac{\xi^D \Gamma(D/2)}{2} \left(1 - \frac{D \xi^2 q^2}{12} + \dots\right). \quad (24)$$

This equation is easily obtained from the power series for the confluent hypergeometric functions. The radius of gyration will be defined for the Gaussian correlation function by

$$R_g^2 = \frac{D \xi^2}{4}. \quad (25)$$

The power model has the small- q expansion

$$I(q) = a^D B(D, 1 + \mu) \times \left(1 - \frac{a^2 D (1+D) q^2}{6 (1+D+\mu) (2+D+\mu)} + \dots \right), \quad (26)$$

where $B(D, 1 + \mu)$ is the Beta function. The radius of gyration for the power model is given by

$$R_g^2 = \frac{a^2 D (D+1)}{2 (1+D+\mu) (2+D+\mu)}. \quad (27)$$

The modified power model has the small- q expansion

$$I(q) = a^D B(D, D) \left(1 - \frac{a^2 (1+D) q^2}{12 (2D+1)} + \dots \right). \quad (28)$$

The radius of gyration for the modified power model is given by

$$R_g^2 = \frac{a^2 (D+1)}{4 (2D+1)}. \quad (29)$$

As mentioned previously, the scattering intensity is determined by the mass scaling dimension D for $R_g^{-1} \leq q \leq 1$. Here we present asymptotic expansions of $I(q)$ for large values of q for the pair-correlation functions in this work. The exponential pair-correlation function yields $I(q)$ with the asymptotic q expansion

$$I(q) \sim \Gamma(D-1) \left[\frac{\sin(\frac{\pi(D-1)}{2})}{q^D} - \frac{(D-1) \cos(\frac{\pi(D-1)}{2})}{\lambda q^{D+1}} + \dots \right]. \quad (30)$$

This expression shows that $I(q) \sim q^{-D}$ for $D < 3$, but that Porod dependence, $I(q) \sim q^{-4}$, is found for $D = 3$. The fractal-region scattering does not exhibit any oscillations for the exponential pair-correlation model. Even simpler expressions can be found for the scattering intensity when D is an integer. An interesting implication of Eq. (30) is that it effectively requires that $D \leq 3$. For $D = 3 + x$ where ($0 \leq x \leq 1$) it is easy to show that $I(q)$ will be negative for $q > (2+x) \cot(\pi x/2)/\lambda$. For large λ , x must be very small to have positive $I(q)$ for $q = 1$. D can be greater than 3 only for relatively small clusters.

The asymptotic expansion of $I(q)$ for the Gaussian correlation function (Ref. 25, p. 508) has two distinct forms for the case that $D < 3$ and for the case that $D = 3$:

$$I(q) \sim \frac{2^{D-2} \sqrt{\pi}}{\Gamma(3/2 - D/2)} \left(\frac{1}{q^D} + \frac{D(D-1)}{\xi^2 q^{D+2}} + \dots \right), \quad (31)$$

for $D < 3$,

and

$$I(q) \sim \frac{\xi^3 \Gamma(3/2)}{2} \exp\left(-\frac{\xi^2 q^2}{4}\right), \quad \text{for } D = 3. \quad (32)$$

Once again the scattering has no oscillations and decreases as q^{-D} for $D < 3$. We note that Porod scattering is not found for $D = 3$, but the scattering intensity decreases as a Gaussian for all q . In fact, the scattering precisely obeys Guinier's exponential approximation

$$I(q) = I(0) \exp(-R_g^2 q^2 / 3). \quad (33)$$

The lack of q^{-4} dependence for $D = 3$ is not surprising because $f'(0) = 0$ for the Gaussian. Porod behavior is only expected for $f'(0) < 0$.

The three-parameter power-law correlation function produces a complicated form for the scattering as seen in Eq. (20). The large- q asymptotic form for this equation is derived from the limiting form of the confluent hypergeometric function (Ref. 25, p. 508) and entails some work to finally arrive at the following form:

$$I(q) \sim A(f_p + f_0), \quad (34)$$

where

$$f_p = \frac{\Gamma(D-1)}{\Gamma(\mu+1)} \left(\frac{\sin(\frac{\pi(D-1)}{2})}{q^D} - \frac{\mu(D-1) \cos(\frac{\pi(D-1)}{2})}{a q^{D+1}} + \dots \right), \quad (35)$$

$$f_0 = \frac{\sin(\frac{2aq - \pi(\mu+1)}{2})}{a^{\mu-D+2} q^{\mu+2}} + \frac{(\mu+1)(D-2) \cos(\frac{2aq - \pi(\mu+1)}{2})}{a^{\mu-D+3} q^{\mu+3}} + \dots, \quad (36)$$

and

$$A = \Gamma(\mu+1). \quad (37)$$

These equations show that the power-law correlation function can result in oscillatory fractal scattering. The spanning length a determines the wavelength of the oscillations. Porod scattering is found for $D = 3$, and the scattering decreases as q^{-D} for $D < 3$ in the fractal region. Equation (35) also limits D to be less than or equal to 3, and the analysis presented above for the exponential correlation function is easily applied to this case.

For completeness the f_p , f_0 , and A terms for the modified power-law correction function are

$$f_p = \frac{1}{D-1} \left(\frac{\sin(\frac{\pi(D-1)}{2})}{q^D} - \frac{(D-1)^2 \cos(\frac{\pi(D-1)}{2})}{a q^{D+1}} + \dots \right), \quad (38)$$

$$f_0 = \frac{\sin(\frac{2aq - \pi D}{2})}{a q^{D+1}} + \frac{D(D-2) \cos(\frac{2aq - \pi D}{2})}{a^2 q^{D+2}} + \dots, \quad (39)$$

and

$$A = \Gamma(D). \quad (40)$$

If $D < 3$, the ratio of the oscillatory terms f_0 to the nonoscillatory terms f_p is proportional to q^{-1} . Hence the oscillations will appear to damp out as q increases. However, the oscillatory and nonoscillatory terms have the same leading q dependence for $D = 3$. Again D cannot be greater than 3 except for small clusters.

It is interesting to note that no oscillations will be observed for $D = 2$ with the modified power correlation function. In this case the scattering intensity for all q is

$$I(q) = \frac{1}{q^2} \left(1 - \frac{\sin(aq)}{aq} \right). \quad (41)$$

The derivative of $I(q)$ with respect to q is thus given by

$$\frac{dI(q)}{dq} = \frac{-1}{q^3} \left(2 + \cos(aq) - \frac{3 \sin(aq)}{aq} \right). \quad (42)$$

This derivative is never positive, and so the scattering must have a monotonic decrease with increasing q .

It is also interesting to note that the nonoscillatory part of the asymptotic scattering intensity is the same to terms $O(q^{-3})$ for all of the correlation functions when $D = 2$. This common asymptotic intensity is $I(q) \sim q^{-2}$. This fact coupled with the absence of oscillations for the power functions indicates that the fractal scattering for $D = 2$ is insensitive to the form of $f(r)$. It is easy to show that this will be true for all $f(r)$ for $D = 2$. In this case the scattering intensity is given by

$$I(q) = \frac{1}{q} \int_0^a f(r) \sin(qr) dr. \quad (43)$$

For $f(0) = 1$ and $f(a) = 0$, integration by parts gives the result that

$$I(q) = \frac{1}{q^2} + \frac{f'(a) \sin(aq)}{q^3} - \frac{1}{q^4} \int_0^{aq} f''(z/q) \sin(z) dz. \quad (44)$$

Hence we see that for D near 2 all $p(r)$ will provide the same fit to the scattering in the fractal region provided the physically reasonable situation that $f'(a)/q$ is small. Different $p(r)$ will provide different quality of fit only for smaller q . The fractal region will yield detailed $f(r)$ information only for $2 < D < 3$.

A simple expression also results for $D = 3$ for the modified power law. Now the scattering intensity for all q is

$$I(q) = \frac{2}{aq^4} \left(2 + \cos(aq) - \frac{3 \sin(aq)}{aq} \right). \quad (45)$$

This equation explicitly shows the Porod scattering and the undamped oscillations for this case.

IV. CLUSTER GENERATION

To test the usefulness of the proposed $p(r)$ to describe the small-angle scattering of fractal clusters, we have calculated the coordinates of the atoms for a variety of clusters with $1.7 \leq D \leq 3$. We calculated synthetic small-

angle scattering for the computer-grown random clusters using the Debye sum. The scattering expected from the different $p(r)$ is then fitted to the synthetic spectra. To provide valid tests we have used a variety of cluster-growth algorithms that produce clusters with different dimensions. Eden,¹⁵ ballistic,¹⁶ and dielectric-breakdown (DBM) [Refs. 17, 18, and 19 (p. 151)] models are used to produce compact $D = 3$ clusters in three-dimensional Euclidean space and $D = 2$ clusters in two-dimensional Euclidean space. Clusters with $D < 3$ in three-dimensional space and $D < 2$ in two-dimensional space are produced with diffusion-limited-aggregation (DLA) [Refs. 13 (pp. 134–181), 3, 5, and 14] dielectric-breakdown, and true self-avoiding random-walk (TSAW) models.

We chose to grow Eden clusters with the method that Vicsek calls variant C (Ref. 13, p. 184). In this cluster-growth model the location for addition of a particle is determined by first randomly choosing an occupied cluster position and then randomly choosing between any vacant sites that are adjacent to the targeted occupied site. If no perimeter sites are found, a new occupied site is chosen to repeat the algorithm. It is apparent that the Eden model produces compact clusters, because the probability of occupying a vacant perimeter site is proportional to the number of occupied sites surrounding it. In three dimensions, the probability of occupying a site in the interior of the cluster may be as much as 6 times the probability of occupying a site on the surface of the cluster. The clusters have $D = 3$ with fuzzy surfaces. The clusters are rapidly grown on a computer.

The ballistic growth model adds particles by starting trajectories at random toward the cluster from a spherical boundary enclosing the cluster. If the trajectory intercepts an occupied site, the particle is added to the last perimeter site before the collision. The clusters have $D = 3$, but have a different structure than the Eden clusters. The ballistic clusters tend to have radial voids because of the shadowing effects of previously occupied sites. The ballistic clusters are also rapidly grown with a simple computer program. Ballistic clusters have D equal to the dimension of Euclidean space in which they are grown and have a self-affine surface. The ballistic cluster is not a fractal³² in the sense that it is not a self-similar structure, but it does show nontrivial scaling behavior.

The DLA model uses a random-walk method to choose the location for the addition of a particle. The additional particle is started on a spherical boundary surface that comfortably surrounds the cluster. The particle is forced to execute a random walk in Euclidean space, and the location for addition is determined if the random walk intercepts a perimeter site. DLA clusters have $D \sim 2.5$ in three-dimensional space, but they are multifractals (Ref. 13, pp. 48–51) and can be described by a tangential and radial pair-correlation function that is indicative of the anisotropic nature of the diffusion-limited aggregate.¹⁴ The DLA clusters are not difficult to grow, but they need large computer memory to efficiently search for possible attachment positions.

The true self-avoiding random-walk model produces a cluster with $D = 2$ that is grown in three-dimensional

Euclidean space. The model produces the cluster by occupying all points of the trajectory of a random walk that is constrained to never intercept itself. The computations are simple, but must be performed on a very large lattice to avoid hitting the walls. Eventually the growth will terminate when the random walker finds itself surrounded by occupied sites.

The DBM model solves the Laplace equation in two or three dimensions to generate the probabilities for the addition of particles according to the rules set forth by Niemeyer, Pietronero, and Wiesmann.¹⁷ The DBM model (Ref. 19, p. 151) uses an adjustable parameter η , which when increased from 0 to 1 produces structures with fractal dimensions D between 3 and ~ 2.5 . The Laplace equation $\nabla^2\phi=0$ for the potential ϕ at each cubic

lattice point in three dimensions is solved with the classic Jacobi method. The boundary conditions are that the potential at each occupied site be 0, and that the potential on a spherical surface surrounding the cluster be 1. The size of the spherical boundary is chosen to be much larger than the size of the cluster to be grown so that no directional anisotropy is observed during the growth process.

In the Jacobi method the potential at each lattice point (i, j, k) which is not an occupied site or a part of the spherical boundary is replaced with the average of the potential at the six surrounding points. The procedure is repeated until the potential converges at the perimeter sites for the cluster. The equation for this process is the following:

$$\phi_{ijk} \leftarrow \phi_{ijk} + \frac{1}{6}(\phi_{i+1jk} + \phi_{i-1jk} + \phi_{ij+1k} + \phi_{ij-1k} + \phi_{ijk+1} + \phi_{ijk-1} - 6\phi_{ijk}). \quad (46)$$

In this equation \leftarrow indicates “replaced by.” The computation of a cluster begins with one occupied site at the center of the spherical boundary surface and with the potential at the other lattice sites set to 0.5. Once the potential ϕ_p at the N_p perimeter sites has been obtained, the probability for addition of the next particle at a perimeter site is given by

$$P(p) = \frac{\phi_p^\eta}{\sum_{p=1}^{N_p} \phi_p^\eta}. \quad (47)$$

After placing the particle, the potential of the new occupied site is fixed at zero and the procedure is repeated. At sites where the potential is not fixed, ϕ is not reset to 0.5 before starting subsequent iterations. Efficient algorithms can be used³³ for producing DBM clusters with integer values for η .

The fractal dimension D of DBM aggregates can be approximated with a mean-field theory.³⁴ The parameters of the mean-field model are D_s , D_w , and η , which correspond to the dimensions of the space and the random walker on the surface and the growth exponent of the DBM model, respectively. A simple formula results for the fractal dimension:

$$D = \frac{D_s^2 + \eta(D_w - 1)}{D_s + \eta(D_w - 1)}. \quad (48)$$

For DBM clusters grown in a three-dimensional (3D) space, $D_s=3$ and $D_w=2$ are the correct parameter values. Recently a fixed scale transformation (FST) theory^{35,36} has been introduced to calculate the fractal dimension and multifractal properties of DBM clusters. The first implementations³⁶ of the theory were applied to analyze DBM clusters grown in 2D space,³⁷ and the results showed that the theory fails to reproduce the fractal dimensions for $\eta \leq 1$, but gives good results for larger η . The theory has been most recently extended to 3D clusters, and the results for the integer η correspond well

with the experiments.³³

For $\eta = 0$ all perimeter sites including those with completely occupied adjacent points have the same probability for addition. This leads to $D = 3$, and this cluster has the same growth algorithm as the Eden growth variant A described by Vicsek (Ref. 13, p. 183). However, the DBM clusters with $\eta = 0$ are different than Eden clusters grown using variant C . The DBM clusters tend to have more unoccupied interior points because the probability for occupation of these is not encouraged by having more occupied neighbors. The $\eta = 0$ clusters tend to add particles at their surfaces until the number of unoccupied interior points is comparable to the number of surface sites. The terms “interior” and “surface” are loosely used here, but a more precise distinction is possible by classifying sites as surface or interior based on the number of occupied neighbors. Interior sites can have four or more occupied neighbor sites, and surface sites can have less. For $\eta = 1$ the clusters are fractal with $D \sim 2.5$ because additional particles will add at perimeter sites where the potential is greatest. This will occur at the surface of the cluster where there are few occupied sites between the perimeter site and the charged spherical boundary surface. There will be no chance for addition at a point completely surrounded by occupied sites.

Although the DLA model is described above as a random-walk process, it is based on diffusion of particles to a cluster. Hence DLA clusters are also obtained from solutions to the Laplace equation. However, the DLA and the DBM ($\eta = 1$) models differ in their boundary conditions. In the DBM model the potential values at the perimeter sites are allowed to vary. In the DLA model the perimeter potential is also fixed at zero, so that the probability for addition of particles is determined by unoccupied sites adjacent to perimeter sites. This phenomenon leads to a well-studied screening effect for DLA.³⁸ These differences in the pair correlation functions due to this change in boundary conditions have been well studied by Turkevich and Scher,³⁹ Ball *et al.*,⁴⁰ and Plischke and Rätz.⁴¹

The DBM model for $\eta > 0$ involves a large amount of computation to solve the Laplace equation for the addition of each particle, because the radius of the boundary surface is typically greater than 100 lattice spacings. Hence the Jacobi algorithm must be applied at 8 000 000 lattice points for each iteration of the method. Since an average of about 50 iterations is required for each Laplace equation solution after the first one, there are about 400×10^6 floating-point operations for each particle in the final cluster. This is a prohibitively large computational problem on a scalar computer. We have found

$$\phi_{ijk} = \phi_{ijk} + \frac{1}{6} b_{ijk} (\phi_{i+1jk} + \phi_{i-1jk} + \phi_{ij+1k} + \phi_{ij-1k} + \phi_{ijk+1} + \phi_{ijk-1} - 6\phi_{ijk}). \quad (49)$$

This simple method removes all conditional and branching statements, and leaves only simple floating-point operations within loops of long length. The program achieves more than 180 Mflops on a single processor of the Cray Y/MP. With this efficient program we can set strict convergence criteria for the potential at the perimeter sites.

V. RESULTS

We fit the parameters of each pair-correlation function to the synthetic-diffraction data by a nonlinear least-squares method. The exponential, Gaussian, and modified power law are two-parameter fits (D and λ , ξ , or a), and the other power law is a three-parameter fit (D , a , μ). $I(q)$ values are obtained for each cluster at 270 values of q which are equally spaced in the range of $\log_{10} q$ from -3 to 0 . Since a major point of this paper is to compare the effectiveness of different $p(r)$ in reproducing small-angle scattering data, the fits are done for $I(q)$ calculated for only a single cluster of each type. Because we do not have $I(q)$ for several random clusters, standard deviations for each $I(q)$ point are not available. Hence *unweighted* least-squares analysis are done. The χ^2 and the standard deviations presented in the tables correspond to this assumption. The χ^2 are not reduced χ^2 that are useful for quality-of-fit arguments. The results of this work are presented in Figs. 1–12 and Tables I–VI. Figures 1–6 show the Debye-sum scattering intensity and the fits for the four correlation functions. The data are presented as log-log plots to indicate scattering that varies by several orders of magnitude. Figures 7–12 give the actual correlation functions for the clusters and the power correlation functions that provide the best fit to the Debye scattering. Because the cluster-correlation functions have many zeros due to their growth on cubic lattices, their graphical presentations have been binned to provide smooth curves. The binning algorithm simply places all pair correlations in the range $i \leq r < i+1$, for i an integer, into a bin centered at $r = i + \frac{1}{2}$. The distances r are normalized by the actual spanning length a , which is the largest pair distance obtained from the cluster co-

ordinates. The pair correlations $p(r)$ are normalized by their maximum values. Since the actual spanning lengths are larger than the spanning lengths for the fits (see Table VI), both powers $p(r)$ appear to terminate for $r/a < 1$. The actual spanning lengths are large, because there is a long but small-amplitude tail in the pair-distance distribution.

The rest of this section is a detailed presentation of the results. For each cluster the overall quality of the fit is discussed by reference to its χ^2 and its fit to the Guinier and fractal regions. The presence of undamped oscillations, the fitting of R_g , the value of D , the size of the spanning lengths, agreement of μ with $D - 1$, and the fit of the correlation functions for different values of r/a are also considered. In some cases χ^2 is not the best criterion for the quality of the fit. In particular, the χ^2

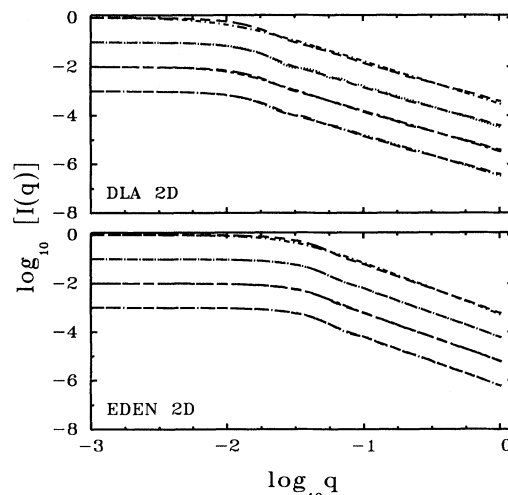


FIG. 1. Fits to the small-angle scattering for DLA (top panel) and Eden (bottom panel) clusters of 10 000 atoms grown on a plane (2D). The Debye scattering is given by dashed lines for each fit. The exponential (dot-dashed lines) fit is the topmost data in each panel. The Gaussian fit (dotted lines) is displaced down by $1 \log_{10}$ unit. The power fit (long-short-dashed lines) is further displaced by $1 \log_{10}$ unit. The modified power fit (long-dash-triple-dotted lines) is the bottom data in each panel.

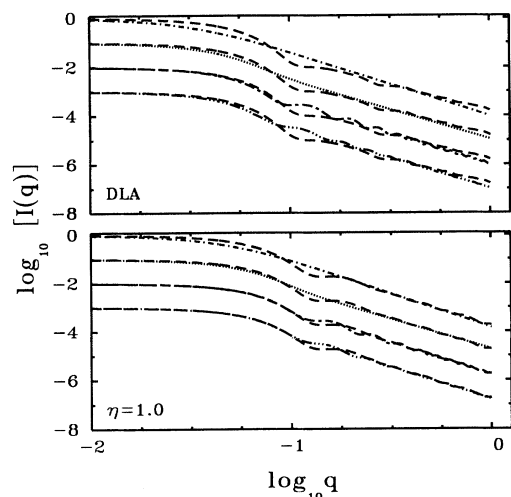


FIG. 2. As in Fig. 1 but for a DLA (top panel) cluster of 25 000 atoms and a DBM ($\eta=1.0$) (bottom panel) cluster of 25 000 atoms.

for a fit that is good for small and intermediate q may have a larger χ^2 if the $p(r)$ give pronounced oscillations for large q .

Figure 1 presents the Debye sum and fits for the four correlation functions for Eden and DLA clusters with 10 000 atoms grown on a plane. The scattering from two-dimensional Eden clusters is perfectly fit by the three-parameter power law. Although the other correlation functions also have very good χ^2 values, the power law is decidedly the best because all inflections and detail are perfectly reproduced. All of the correlation functions provide excellent fits in the fractal region, but differ for smaller q . This is consistent with the discussion for $D = 2$ scattering presented previously. The exponential correlation function provides the poorest fits, and its failure

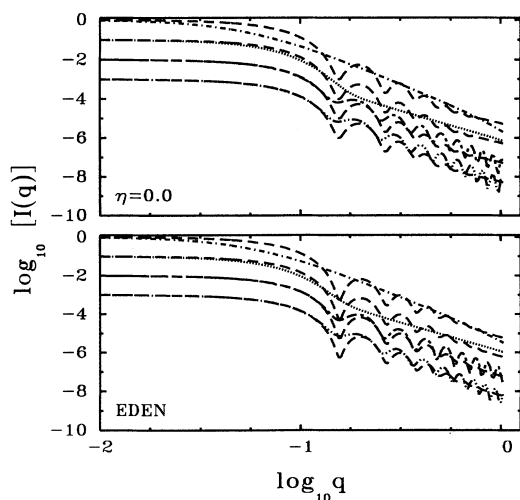


FIG. 3. As in Fig. 1 but for an Eden (bottom panel) cluster with 100 000 atoms and a DBM ($\eta=0.0$) (top panel) cluster of 100 000 atoms.

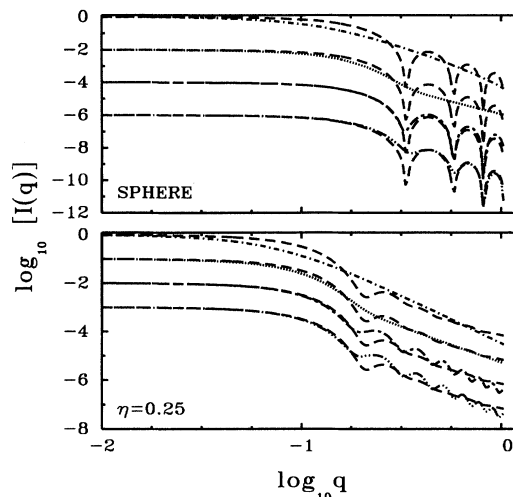


FIG. 4. As in Fig. 1 but for a sphere (top panel) with 10 000 atoms and a DBM ($\eta=0.25$) (bottom panel) cluster with 25 000 atoms.

in the Guinier region leads to inaccurate R_g values. The power-law models provide R_g that have errors less than 4%, while the R_g for the Gaussian model is accurate to within 7%. Figure 1 also shows that the exponential model provides the poorest fits for DLA clusters grown in two-dimensional space, while the other $p(r)$ provide good fits. The power laws provide much better R_g values than the Gaussian or exponential models.

Eden clusters in Euclidean two-space have trivially $D=2$. This result is confirmed by mean-field theory.³⁴ We obtain $D=2.01$ from the three-parameter power model and $D=1.99$ for the two-parameter power model. The Gaussian and exponential models have $D=2.14$ and $D=1.96$, respectively. Since the Eden cluster is a compact cluster with a fractal surface, we would expect that good analysis of the scattering should yield a value for D

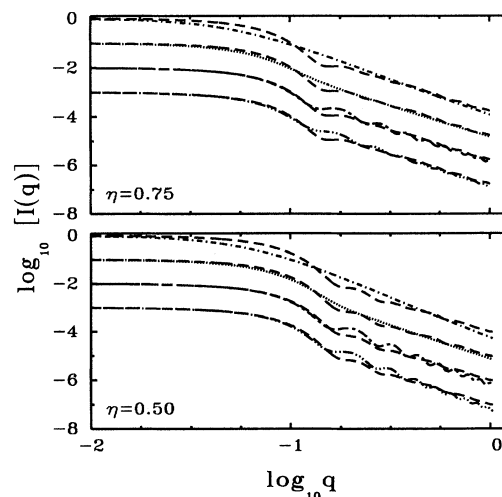


FIG. 5. As in Fig. 1 but for DBM ($\eta=0.5$) (bottom panel) and DBM ($\eta=0.75$) (top panel) clusters with 25 000 atoms.

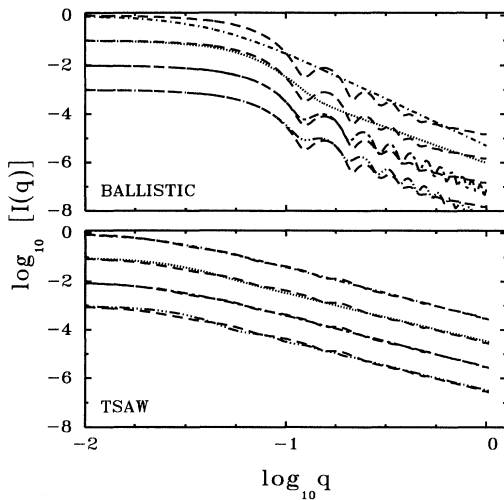


FIG. 6. As in Fig. 1 but for a ballistic (top panel) cluster with 100 000 atoms and a TSAW (bottom panel) polymer with 18 500 atoms.

of 2 or slightly less.

Numerical experiments⁵ on DLA clusters in Euclidean two-space have found $1.66 \leq D \leq 1.70$ for clusters with less than 10 000 particles. The larger value for D is found from the dependence of $\ln R_g$ vs $\ln N$ and the lower from an analysis that is equivalent to determining the dependence of $\ln[p(r)]$ vs $\ln r$. The most accurate value is considered to be $D = 1.715 \pm 0.004$.³³ Mean-field theory³⁴ gives $D=1.67$. The power-law correlation functions provide best-fit values of $D=1.68$, which is the midrange

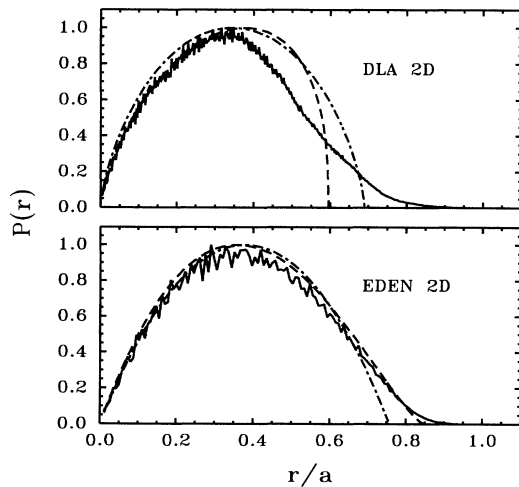


FIG. 7. Correlation functions for DLA (top panel) and Eden (bottom panel) clusters of 10 000 atoms grown on a plane (2D). The actual pair-correlation function (solid lines) has been averaged over a small range of r to remove severe oscillations caused by the nonallowed distances on a lattice. The fitted power correlation function (dashed lines) and the fitted modified power correlation function (long-short dashed lines) are also given. The distances are scaled to the spanning length a of the actual cluster.

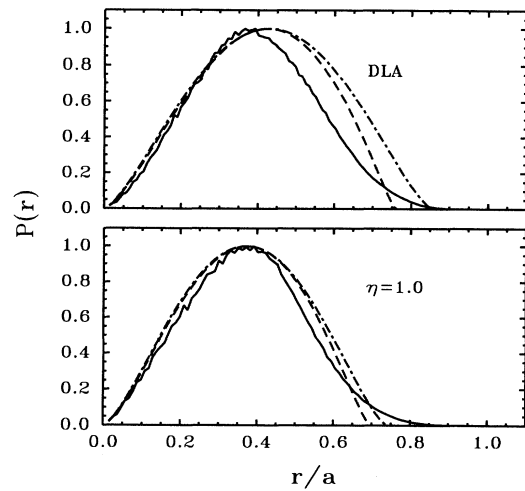


FIG. 8. As in Fig. 7 but for a DLA (top panel) cluster of 25 000 atoms and a DBM ($\eta=1.0$) (bottom panel) cluster of 25 000 atoms.

of the experimentally determined values. The Gaussian and exponential models yield $D=1.66$ and $D=1.77$, respectively. Clearly the exponential fails to fit any experimental or theoretically known values.

The pair-correlation functions for the clusters in Fig. 1 are shown in Fig. 7. The bottom panel demonstrates that the actual correlation function and the three-parameter power function are virtually identical for a 2D Eden cluster. The two-parameter power-law correlation function falls off too steeply at large r values compared with the actual $p(r)$, but the corresponding $I(q)$ agree well. The top panel in Fig. 7 shows that the power functions are not suitable for reproducing the long-range order found in two-dimensional DLA clusters. The infinite slopes at the largest r are not physical. However, the result in q

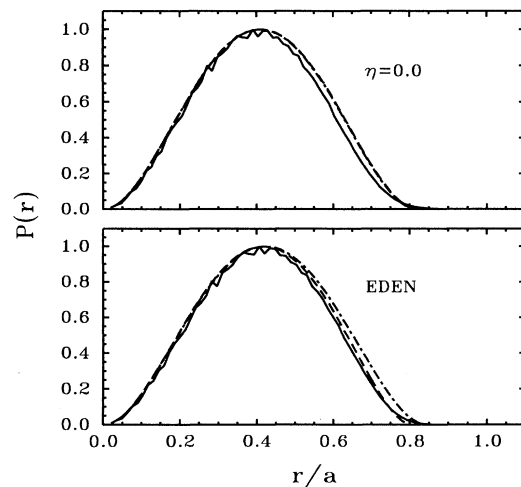


FIG. 9. As in Fig. 7 but for an Eden (bottom panel) cluster with 100 000 atoms and a DBM ($\eta=0.0$) (top panel) cluster of 100 000 atoms.

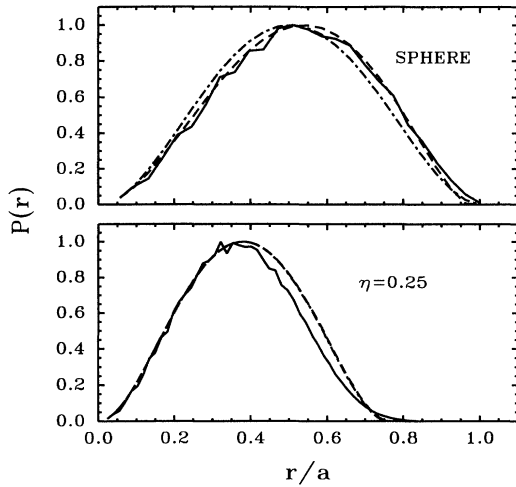


FIG. 10. As in Fig. 7 but for a sphere (top panel) with 10000 atoms and a DBM ($\eta=0.25$) (bottom panel) cluster with 25000 atoms.

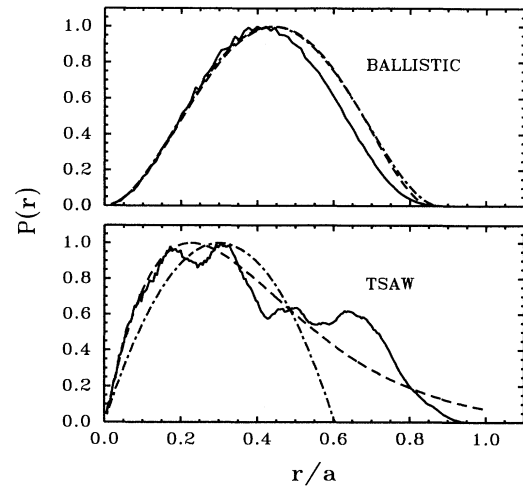


FIG. 12. As in Fig. 7 but for a ballistic (top panel) cluster with 100000 atoms and a TSAW (bottom panel) polymer with 18500 atoms.

space from Fig. 1 appears to be excellent. From a review of Tables I–V it can be seen that only the power-law models and the Gaussian can reproduce the known literature value of the fractal dimension, and only the power laws reproduce the R_g of the cluster well. For two-dimensional clusters even gross errors in the correlation function do not give rise to substantial χ^2 errors in the fitting of $I(q)$. However, reasonably large errors in the fitted parameters can occur when using the exponential model.

Figure 2 presents the Debye sum and fits for DLA and DBM ($\eta = 1$) clusters with 25000 atoms grown in three-dimensional space. For the DBM cluster only the power-law models provide an excellent fit to the Guinier region and partially reproduce the transitory local minima found just before the fractal region. The Gaussian model provides a poorer fit, and the exponential model gives the

worst fit for the Guinier region. All of the models provide good fits in the fractal region. For the DLA cluster the exponential and Gaussian models fail to fit the Guinier region, and the power models do a better job, but not as good as for the DBM $\eta = 1$ cluster. For DLA clusters $I(q)$ has a local minimum near $q = 0.1$ that is not well fit by any of the models. The power models pro-

TABLE I. Exponential pair-correlation fits to small-angle scattering. Size is the number of atoms in the cluster. D and λ are defined in Eq. (18). σ_D and σ_λ are standard errors. χ^2 is the estimated variance.

Cluster	Size	D	σ_D	λ	σ_λ	χ^2
ballistic	100k	2.989	0.011	22.19	0.53	0.0497
dla	100k	2.474	0.025	55.56	2.19	0.0393
dla	25k	2.526	0.025	28.68	0.98	0.0246
dla	10k	2.518	0.027	21.71	0.76	0.0222
dla2d ^a	10k	1.767	0.010	109.01	2.15	0.0046
dla	5k	2.574	0.026	15.17	0.46	0.0156
eden	100k	3.043	0.008	17.70	0.42	0.0679
eden	10k	3.128	0.015	7.46	0.19	0.0458
eden2d ^a	10k	2.141	0.009	31.45	0.41	0.0020
eden	5k	3.186	0.017	5.57	0.14	0.0327
DBM 0.0 ^b	100k	3.047	0.006	18.71	0.42	0.0693
DBM 0.25 ^b	25k	2.996	0.015	12.46	0.30	0.0318
DBM 0.5 ^b	25k	2.855	0.019	14.82	0.39	0.0228
DBM 0.75 ^b	25k	2.702	0.020	18.32	0.49	0.0173
DBM 1.0 ^b	25k	2.636	0.016	19.67	0.41	0.0094
offdla2d ^{a,c}	10k	1.759	0.011	111.72	2.59	0.0063
offdla ^c	10k	2.514	0.035	22.51	1.04	0.0395
TSAW	18k	2.140	0.004	42.70	0.27	0.0006
sphere	10k	3.135	0.022	7.65	0.32	0.1345
sphere	5k	3.244	0.014	5.40	0.18	0.1117

^aCluster grown in two-dimensional space.

^bThe number following “DBM” is the value for η .

^cThe prefix “off” signifies that the cluster is produced off lattice.

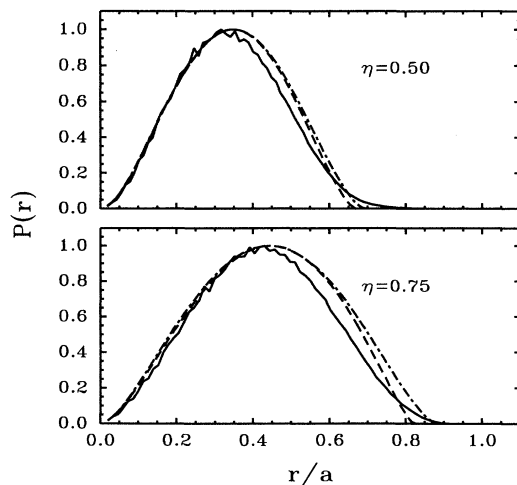


FIG. 11. As in Fig. 7 but for DBM ($\eta=0.5$) (top panel) and DBM ($\eta=0.75$) (bottom panel) clusters with 25000 atoms.

TABLE II. Gaussian pair-correlation fits to small-angle scattering. D and ξ are defined in Eq. (19). σ_ξ and σ_D are standard errors.

Cluster	Size	D	σ_D	ξ	σ_ξ	χ^2
ballistic	100k	2.890	0.005	38.67	0.48	0.0186
dla	100k	2.394	0.015	98.07	2.17	0.0191
dla	25k	2.398	0.013	53.75	0.91	0.0097
dla	10k	2.376	0.014	41.14	0.70	0.0090
dla2d	10k	1.663	0.004	189.04	1.37	0.0009
dla	5k	2.391	0.012	30.02	0.40	0.0053
eden	100k	2.918	0.006	31.90	0.53	0.0405
eden	10k	2.888	0.007	15.06	0.20	0.0192
eden2d	10k	1.957	0.002	61.85	0.17	0.0002
eden	5k	2.874	0.007	11.95	0.13	0.0120
DBM 0.0	100k	2.943	0.004	31.51	0.44	0.0347
DBM 0.25	25k	2.825	0.006	24.02	0.22	0.0074
DBM 0.5	25k	2.687	0.007	29.01	0.28	0.0050
DBM 0.75	25k	2.527	0.009	36.38	0.39	0.0047
DBM 1.0	25k	2.430	0.008	40.51	0.39	0.0032
offdla2d	10k	1.659	0.005	192.14	1.89	0.0017
offdla	10k	2.399	0.021	41.44	1.08	0.0218
TSAW	18k	1.969	0.008	82.99	0.96	0.0028
sphere	10k	2.907	0.013	15.18	0.42	0.0995
sphere	5k	2.905	0.014	12.05	0.32	0.0872

duce an oscillatory component that is out of phase with the minima seen in the Debye data, but this oscillatory component may be facilitating the fit in other cases. Although the figures show that DLA clusters are not well fit in either real or q spaces, the three-parameter power model still produces the correct value of D and gives R_g within 10%. This is not true of the other models that fail quite badly in reproducing D or the proper R_g . The modified power model also provides a better fit than either the exponential or Gaussian. The slight oscillations

in the fits properly damp out for large q . It is interesting to note that the scattering intensity for all of the fits decreases more quickly than the Debye sum in the fractal region.

The fractal dimension of DLA clusters in Euclidean three-space has been extensively studied. Numerical experiments² on 16 unique DLA clusters of varying size find values of D between 2.25 and 2.64 using a radius of gyration analysis on the last 90% of the points added to the clusters. The average value of $D=2.49$ was found us-

TABLE III. Power-law pair-correlation fits to small-angle scattering. D , μ , and a are defined in Eq. (20). σ_D , σ_μ , and σ_a are standard errors.

Cluster	Size	D	σ_D	a	σ_a	μ	σ_μ	χ^2
ballistic	100k	2.969	0.004	73.70	0.97	1.80	0.02	0.01715
dla	100k	2.466	0.016	157.46	1.44	1.15	0.07	0.02510
dla	25k	2.484	0.014	85.99	0.72	1.16	0.05	0.01222
dla	10k	2.448	0.017	70.66	1.01	1.29	0.07	0.01214
dla2d	10k	1.672	0.004	243.93	1.19	0.47	0.02	0.00094
dla	5k	2.470	0.016	54.75	0.99	1.46	0.08	0.00736
eden	100k	2.996	0.004	58.27	0.12	1.84	0.03	0.03117
eden	10k	2.997	0.007	26.58	0.09	1.79	0.03	0.01645
eden2d	10k	2.011	0.001	112.58	0.19	1.38	0.01	0.00001
eden	5k	3.005	0.008	21.81	0.10	1.86	0.03	0.00960
DBM 0.0	100k	3.017	0.004	61.94	0.18	2.01	0.04	0.04423
DBM 0.25	25k	2.948	0.006	44.96	0.21	1.86	0.03	0.01133
DBM 0.5	25k	2.797	0.007	51.32	0.21	1.55	0.03	0.00571
DBM 0.75	25k	2.626	0.009	62.04	0.35	1.37	0.03	0.00484
DBM 1.0	25k	2.527	0.007	68.59	0.35	1.32	0.03	0.00218
offdla2d	10k	1.666	0.005	231.57	0.95	0.35	0.02	0.00166
offdla	10k	2.505	0.021	61.27	0.56	1.06	0.06	0.02604
TSAW	18k	2.118	0.005	881.05	67.59	18.28	1.60	0.00061
sphere	10k	2.953	0.003	25.73	0.02	1.56	0.01	0.02220
sphere	5k	2.947	0.004	20.38	0.02	1.54	0.01	0.01693

TABLE IV. Modified power-law pair-correlation fits to small-angle scattering. D and a are defined in Eq. (21). σ_D and σ_a are standard errors.

Cluster	Size	D	σ_D	a	σ_a	χ^2
ballistic	100k	2.984	0.003	75.99	0.24	0.0194
dla	100k	2.441	0.015	182.41	2.90	0.0252
dla	25k	2.478	0.013	97.32	1.13	0.0128
dla	10k	2.444	0.014	75.12	0.90	0.0121
dla2d	10k	1.679	0.003	269.31	1.27	0.0009
dla	5k	2.470	0.012	54.83	0.52	0.0073
eden	100k	3.011	0.002	61.29	0.18	0.0375
eden	10k	3.030	0.003	28.06	0.11	0.0192
eden2d	10k	1.988	0.002	100.27	0.18	0.0002
eden	5k	3.035	0.003	22.46	0.08	0.0103
DBM 0.0	100k	3.018	0.002	61.83	0.14	0.0440
DBM 0.25	25k	2.957	0.004	45.81	0.20	0.0117
DBM 0.5	25k	2.814	0.006	54.88	0.30	0.0069
DBM 0.75	25k	2.640	0.008	66.82	0.44	0.0056
DBM 1.0	25k	2.534	0.006	73.14	0.36	0.0024
offdla2d	10k	1.673	0.004	274.31	1.70	0.0016
offdla	10k	2.472	0.021	75.43	1.31	0.0266
TSAW	18k	2.003	0.009	134.78	1.19	0.0040
sphere	10k	3.064	0.001	26.73	0.04	0.0564
sphere	5k	3.063	0.001	21.58	0.07	0.0469

ing an average cluster size of 7899 particles. Our 10 000-particle DLA cluster has $D=2.45$ when fit by the three-parameter power model and $D=2.44$ when fit by the two-parameter power model. The Gaussian and exponential models yield $D=2.38$ and $D=2.52$. This cluster is one of the few cases where the Gaussian model fails to provide agreement with the expected experimental or theoretical value. The exponential and power models give very good values for D . Mean-field theory³⁴ predicts $D=2.5$ for DLA clusters in a 3D space. FST theory⁴²

yields $D = 2.49$. Since the fitted $I(q)$ curves have a negative slope that has a larger magnitude than that for the Debye-sum in the fractal region, a simple estimate of D for the Debye-sum data from the slope of the plot of $\ln I(q)$ vs $\ln q$ will be smaller than 2.49. The tables show that the exponential and three-parameter power models give the same D value of 2.51 for an off-lattice DLA cluster in a 3D space. The corresponding modified power and Gaussian fits give $D = 2.47$ and $D=2.40$. The Gaussian correlation function for DLA clusters always gives

TABLE V. Fitted and actual radii of gyration. Actual R_g is the radius of gyration found from coordinate data. R_g in columns 3, 4, 5, and 6 are defined by Eqs. (23), (25), (27), and (29).

Cluster	Size	R_g	R_g	R_g	R_g	R_g Actual
		Exponential	Gauss	Power	Modified Power	
ballistic	100k	54.2	32.9	28.6	28.7	28.5
dla	100k	115.2	75.9	63.9	69.8	58.8
dla	25k	60.5	41.6	34.9	37.2	33.9
dla	10k	45.7	31.7	28.3	28.7	26.8
dla2d	10k	170.5	121.9	101.1	105.6	104.7
dla	5k	32.5	23.2	20.9	21.0	20.3
eden	100k	43.9	27.2	22.6	22.8	22.6
eden	10k	19.0	12.8	10.4	10.6	10.7
eden2d	10k	57.7	43.3	40.3	38.8	40.4
eden	5k	14.4	10.1	8.4	8.5	8.5
DBM 0.0	100k	46.5	27.0	23.4	23.4	23.1
DBM 0.25	25k	30.5	20.2	17.3	17.3	17.4
DBM 0.5	25k	34.8	23.8	20.3	20.8	20.4
DBM 0.75	25k	41.0	28.9	24.7	25.4	24.4
DBM 1.0	25k	43.1	31.6	27.2	27.9	27.8
offdla2d	10k	174.1	123.7	100.5	107.6	105.0
offdla	10k	47.3	32.1	25.5	28.8	25.3
TSAW	18k	78.3	58.2	73.1	52.2	69.1
sphere	10k	19.5	12.9	10.4	10.1	10.5
sphere	5k	14.2	10.3	8.2	8.1	8.3

TABLE VI. Actual and fitted spanning lengths. Actual a is the spanning length from coordinate data. a_{mod} is the spanning length fitted using Eq. (21). a_{mod}/a is the ratio of the fitted to the actual spanning length.

Cluster	Size	Actual a	a_{mod}	a_{mod}/a
ballistic	100k	86.49	75.99	0.878
dla	100k	210.50	182.41	0.866
dla	25k	113.12	97.32	0.860
dla	10k	94.39	75.12	0.795
dla2d	10k	390.28	269.31	0.690
dla	5k	71.81	54.83	0.763
eden	100k	72.03	61.29	0.851
eden	10k	35.64	28.06	0.787
eden2d	10k	132.14	100.27	0.758
eden	5k	29.83	22.46	0.752
DBM 0.0	100k	75.24	61.83	0.821
DBM 0.25	25k	61.20	45.81	0.748
DBM 0.5	25k	67.35	54.88	0.814
DBM 0.75	25k	75.54	66.82	0.884
DBM 1.0	25k	98.78	73.14	0.740
offdla2d	10k	350.90	274.31	0.781
offdla	10k	87.18	75.43	0.865
TSAW	18k	223.65	134.78	0.602
sphere	10k	26.98	26.73	0.990
sphere	5k	21.78	21.58	0.991

a fractal dimension that is not consistent with the other values, except in the 2D case.

The fractal dimension of DBM clusters for varying η values have been experimentally studied¹⁹ where the clusters usually have fewer than 10 000 particles. Mean-field theory predicts $D=2.5$ for $\eta = 1$. FST theory⁴² yields $D = 2.49$. For $\eta = 1$ the DBM and DLA clusters are expected to have the same D . In the cited study a 4000-particle DBM cluster grown with $\eta = 1$ was found to have $D=2.65$, using a radius of gyration analysis. Our 25 000-particle DBM $\eta = 1$ cluster has $D=2.53$ using either of the power models to fit the scattering. The Gaussian and exponential models give $D=2.43$ and $D=2.64$, respectively. The power models agree very well with the mean-field prediction, and experimental studies. Figure 8 shows the pair-correlation functions for DLA and $\eta = 1$ DBM clusters. The actual $p(r)$ are similar for the two clusters, but the fitted $p(r)$ are different. For either cluster the power models agree for r less than the r corresponding to the maximum in $p(r)$. The power functions provide a better fit for DLA clusters at small r and DBM clusters at large r . The power-law correlation functions are broader than the actual in either case.

Figure 3 shows the very similar diffraction patterns of Eden and DBM ($\eta = 0$) clusters with 100 000 particles. The Debye patterns appear superimposable. The power-law models provide the best fits to the Guinier regions for both clusters, and the next best fits are provided by the Gaussian model. The worst Guinier fits are produced with the exponential model. Table III shows that the parameter μ for the three-parameter power fit is different for the two clusters, but D and a are very similar. The power fit to the DBM cluster shows that $\mu = D - 1$, so that there is virtually no difference between the fits (pa-

rameters and χ^2) for the two power models. However, for the Eden cluster, the fact that μ is not equal to $D - 1$ allows a better fit to the Guinier region. This better fit allows the power model to reproduce R_g exactly. It is interesting that the Gaussian model produces the best χ^2 for the DBM cluster, but the power models are much better at obtaining the proper R_g . This demonstrates that χ^2 is not always the best measure in evaluating the results from these models. The power models have better χ^2 for the Eden cluster. The power laws provide some oscillatory fit for both clusters in the q region past the Guinier region, but the oscillations do not damp out as rapidly as the Debye-sum data. It appears that these slowly damped oscillations contribute to the larger χ^2 for the power-law fits. For the Eden cluster the slope of the power and exponential models fit the Debye-sum slope in the fractal region, but the Gaussian model has a negative slope with a magnitude that is too small. For the DBM cluster the Gaussian model has the correct slope, but the other fits have negative slopes with too large a magnitude.

Any DBM cluster grown with a zero growth exponent $\eta = 0$ will have $D=3$ when the clusters are grown on three-dimensional lattices. Both power models give $D=3.02$ for our 100 000-particle $\eta = 0$ cluster. The Gaussian model gives a reasonable value of $D=2.94$. The exponential model gives a value of $D=3.05$. Mean-field theory predicts $D = 3$ for $\eta = 0$ clusters in three-space. The low D value for the Gaussian model is consistent with its negative slope with too small a magnitude for $I(q)$ in the fractal region.

The Eden model produces clusters that are more compact than the DBM $\eta = 0$ clusters, but $D = 3$ for both. The unmodified power model gives a fit of $D=3.00$, while the modified model gives a value of $D=3.01$. The Gaussian and exponential models give D values of $D=2.92$ and $D=3.04$, respectively.

The correlation functions for the clusters in Fig. 3 are shown in Fig. 9. Since the fitted parameters from the power models for the DBM cluster are identical, it is clear that the correlation functions are also identical. The power correlation functions agree well with the real correlation function. R_g is well reproduced, although the power laws give a much smaller spanning length than the actual. The Eden cluster shows subtle differences in fits between the power models. The three-parameter model has a smaller spanning length, but is nearly identical to the actual correlation function. The modified power law has a slightly larger spanning length which causes it to deviate when $r/a > 0.5$. The fact that the unmodified power model is very accurate at large r/a and has $\mu \neq D - 1$ may indicate a subtle difference in the long-range order between Eden and DBM clusters where the latter exhibits exact $\mu = D - 1$ behavior. The deviation of μ from $D - 1$ for the Eden cluster may be a genuine indication of this long-range order.

Figure 4 displays the diffraction space for a sphere and an $\eta=0.25$ DBM cluster. Again the power-law models provide the best fits to the Guinier regions for both clusters. The Gaussian model does not produce as good fits. The worst Guinier region fits are produced with the ex-

ponential model. The power models give almost the same fit for the DBM cluster because μ for the three-parameter power law is very close to $D - 1$. The two power models give the same R_g which agrees well with the actual R_g . The Gaussian model produces the best χ^2 for the DBM cluster, but R_g is not fit well. The exponential model produces the worst χ^2 of any of the models, and the R_g is extremely poor as can be seen from the Guinier region. The Gaussian fits the fractal region very well, but the slopes from the other models have a negative slope with a magnitude that is too large. Also the oscillations in the power fits do not damp out as rapidly as the Debye-sum scattering intensity.

The sphere is fit with much smaller χ^2 using either of the power models, compared to the other models. The power fits show very good R_g and D values and spanning lengths that are very close to the actual spanning length. The three-parameter model has $\mu \simeq 1.55$, instead of $\mu \simeq D - 1$, which is found for some other compact clusters. The three-parameter power model is better than the modified power function in fitting the amplitudes of the oscillations, as well as the region between the Guinier and Porod regions. The phase of the oscillations is better for the two-parameter model, but the depth of the oscillations is not as well fit. The errors in fitting the oscillations are found because the power correlation functions differ from the exact $p(r)$ given in Eq. (15). The extra $1 + r/(2a)$ factor is responsible for producing zeros in $I(q)$ as predicted by Eq. (16).

We have found no work in the literature that considers DBM clusters grown on three-dimensional lattices with $\eta=0.25$. Mean-field theory predicts $D=2.85$, and we obtain $D=2.95$ from the power-model fits. The fits from the Gaussian and the exponential models give $D=2.83$ and $D=3.00$, respectively. The exponential correlation function gives a fractal dimension that is too high. These results are consistent with the magnitudes of the negative slopes of $\ln I(q)$ vs $\ln q$ in the fractal region.

The fractal dimension of a sphere is trivially $D=3$, and an analytically correct correlation function should yield this as a fit to the scattering. However, incorrect correlation functions may give fits with inappropriate parameters because the fitting routine will attempt to minimize the square of the deviations in the presence of deep oscillations. The power correlation functions are only approximations to the correct correlation function of a sphere [Eq. (15)], which underestimate the value of the correlation function as $r \rightarrow a$. The three-parameter power model gives $D=2.95$, and the two-parameter model gives $D=3.06$. Much worse fractal dimensions are obtained with the Gaussian and exponential models, which give $D=2.91$ and $D=3.14$, respectively.

The correlation functions for these clusters are shown in Fig. 10, which demonstrates the difference in the power correlation functions for Euclidean and fractal clusters. Euclidean spheres have symmetrical correlation functions with a sharply defined spanning length. The three-parameter power model reproduces the actual $p(r)$. The two-parameter $p(r)$ is too large at smaller r and too small at large r , but it still provides a good fit to the actual pair-correlation function. The errors are those expected

for the neglected contribution of the $1 + r/(2a)$ factor. The correlation functions presented for the fractal DBM cluster show that the power models can accurately give the small r part of $p(r)$, but have substantial errors for $r \geq 0.4$. The two- and three-parameter power correlation functions are the same for the DBM cluster.

$I(q)$ for DBM clusters with lower fractal dimensionality than the DBM cluster in Fig. 4 are shown in Fig. 5. The Guinier region for both clusters is best fit by the power-law models. The Gaussian model provides better fits to the Guinier region than the exponential model. Both power models appear to provide nearly the same fit, and the χ^2 values only differ by 18%. The power models spanning lengths differ by about 7% from each other for either of the clusters shown. The largest errors for the power models occur around $\log_{10}(q) = -0.8$. This is the transition area between the Guinier region and the fractal region, and is a difficult region to fit for all of the DBM clusters. The Gaussian fits in the top and bottom panels are good except for the Guinier region, which leads to a poor R_g value. For the $\eta=0.75$ cluster in the fractal region, the exponential model provides the worst fit, and the Gaussian provides the best fit. This may account for why the Gaussian has slightly better χ^2 than the power models.

Three-dimensional DBM clusters where $\eta=0.5$ have been studied,¹⁹ with the conclusion that $D=2.78$. This value compares favorably with our three-parameter power fit, which gives $D=2.80$. The two-parameter power model has $D=2.81$, which is also very close. The Gaussian and exponential models give values of $D=2.69$ and $D=2.86$. This would appear to support a trend that the exponential model provides the largest estimates for D , while the Gaussian model provides the lowest estimates. The large D for the exponential is consistent with the magnitude of the negative slope being too large in the fractal region. The mean-field result for this cluster is $D=2.71$, which in this case is very close to the Gaussian fit.

There appear to be no literature results for DBM clusters grown with $\eta=0.75$. Our results from the three-parameter and two-parameter power models are $D=2.63$ and $D=2.64$. These compare well with the expected mean-field value of $D=2.60$. The Gaussian and exponential models give different results from the mean-field value, giving $D=2.53$ and $D=2.70$, respectively. It appears that as the growth exponent ($\eta \rightarrow 1.0$), the χ^2 becomes smaller, while the value of D for both of the power models approaches the mean-field value of D given by Eq. (48).

The correlation functions for these clusters are shown in Fig. 11. The power correlation functions are very similar to each other for the DBM $\eta=0.5$ cluster, and agree with the actual $p(r)$ at small r . The power correlation functions show larger differences from each other for the $\eta=0.75$ cluster, but both provide a reasonable fit to the small r part of $p(r)$. At large r the power correlation functions tend to be larger than the actual.

Figure 6 shows $I(q)$ for a *true self-avoiding random-walk* (TSAW) polymer. The TSAW polymer is a well-studied model.⁴³ This polymer reached a size of about

18500 particles before growth terminated. Figure 6 demonstrates that all of the models fit the fractal region very well, which is expected for a $D = 2$ cluster. The exponential and three-parameter power models have the lowest χ^2 . The Guinier region for the TSAW polymer is not fit well by any of the models, but the best R_g is found with the three-parameter power model. The modified power model is the worst fit of any of the models. The power-function spanning lengths are not reasonable. Only the unmodified power model can predict the real R_g to within 10%. The exponential $p(r)$ is commonly used in the literature for evaluating 2D polymeric type structures, but it appears to be unreliable for the evaluation of the R_g for such structures. The Debye equation⁴⁴ derived for a TSAW polymer, $I(q)/I(0) = 2[\exp(-x) + x - 1]/x^2$, where $x = R_g^2 q^2$, also provides a good fit. The only dilemma should be that any model with an $f(r)$ that damps to any extent will provide a good fit in q space to experimental data. The real test of a model has to lie in its ability to properly evaluate both D and R_g . None of the models appear to be able to follow the very mild oscillations in the Debye data.

Figure 6 also shows the scattering for a ballistic cluster with 100 000 atoms. The Debye data for the ballistic cluster is very similar to that for the Eden and DBM $\eta=0.0$ clusters, and shows the characteristic oscillations associated with clusters whose fractal dimension is very close to $D=3$. The power-law models provide the best fit to the Guinier region, and the next best fit is provided by the Gaussian model. The worst Guinier fit is produced by the exponential model. The fitted χ^2 for the ballistic cluster is better than for either the Eden or the DBM $\eta=0.0$ cluster. This better fit is visible in Fig. 6. It can be seen immediately that the very first large oscillation is best fit by the unmodified power model. Both power models produce excellent R_g values, but the exponential and Gaussian models cannot reproduce the actual R_g because of their poor fits to the Guinier scattering. The power models show oscillations that have good phase agreement with the Debye scattering, but the oscillations in the power scattering do not damp out with increasing q . The oscillations in the scattering damp out more quickly for the two-parameter power correlation function. A more bothersome observation is that in the fractal scattering region, the negative slope of the Debye data has a smaller magnitude than is found for all of the fits. The Debye data decrease approximately as q^{-2} for large q . The ballistic cluster is a good example of why χ^2 may not be a good measure of the fitting ability of the power models. The χ^2 for the three-parameter power model fit of the ballistic cluster is about 8 times larger than the χ^2 for the fit for a DBM $\eta = 1.0$ cluster. But R_g is reproduced to within 0.3% for the ballistic cluster, while R_g is only reproduced within 2% for the DBM cluster. The magnitude of χ^2 for the power models appears to be mostly due to the undamped oscillations, which should not have a large effect on D or R_g . The fitted μ parameter in the three-parameter fit is close to $D - 1$.

In three-dimensional Euclidean space the fractal dimension of the TSAW polymer should have $D=2$, which is the same as that for a random walker.³⁴ Although the

correlation function for the TSAW polymer has several maxima, the D value from the modified power model gives $D=2.00$, while the unmodified power model gives $D=2.12$. The Gaussian and exponential models give $D=1.97$ and $D=2.14$, respectively. The Debye polymer scattering expression⁴⁴ is based on $D = 2$, which is obvious from the asymptotic dependence of $I(q)$. The $D = 2$ dependence for the Debye expression can also be found by taking the sine transform of $qI(q)$ as shown in Eq. (17).

It can be proven (Ref. 13, p. 192) that the fractal dimension of a ballistic cluster is $D = d$, where d is the dimension of the lattice on which the cluster is grown. Our fitting methods are sensitive to the density-correlation function between the voids of the structure and the branches of the structure.⁴⁵ If the amount of void space per unit volume of the structure is constant, then the fractal dimension of the structure should be $D = d$. The fits we obtain with the unmodified and modified power models are $D=2.97$ and $D=2.98$, respectively. The Gaussian and exponential models give $D=2.89$ and $D=2.99$, respectively. The poor agreement for the slope in the fractal region using the exponential model does not appear to cause errors in obtaining the proper fractal dimension. The other models do a better job in reproducing the slope of the Debye-sum scattering.

The correlation functions associated with Fig. 6 are shown in Fig. 12. The actual correlation function for the TSAW polymer is seen to have several maxima. The various maxima are associated with the fact that the TSAW polymer has a number of loops where the random-walk trajectory reversed its direction. In the vicinity of a loop many monomers will have the same distance from monomers near another loop. The modified power $p(r)$ provides a poor fit to the actual correlation function, but it still reproduces the fractal scattering very well. The three-parameter power model provides a good fit for small r and appears to provide a smooth approximation to the actual function at larger r , but the fitted spanning length and μ value are unusual. The two- and three-parameter power correlation functions for the ballistic cluster are nearly identical, and they provide a good fit to the actual correlation function for small r . Both functions become greater than the actual correlation function at $r/a > 0.45$, which is close to the value at which other compact clusters begin to deviate. The actual correlation function and the power models seem to parallel each other at values of $r/a > 0.5$. Figure 12 seems to show that the spanning length of the power models is actually larger than that for the real correlation function. However, this is not the case since the real function has a long and small-amplitude tail that is not visible in Fig. 12.

VI. DISCUSSION

In discussing the idea of fractals and scale invariance it is important to note that any fractal, size, and shape information contained in the real-space coordinates through the actual pair-correlation function must be preserved in the Fourier transform to q space. The q space of

all the aggregates we have examined has been determined by the analog of a Fourier transform of their spatial pair-correlation functions. This principle constitutes Debye scattering and all other diffraction phenomena. We have shown by example that any of our pair-correlation functions can roughly reproduce the fractal dimension with q^{-D} scattering in the fractal region, for $D < 3$. We also have shown that the Guinier scattering and the transition regions before the fractal region are reproduced only with a realistic $f(r)$ such as the power-law function, regardless of the fractal dimension or size of the structure. Because of Fourier reciprocity, we would expect that all models should behave similarly in the fractal region. In reality all models exhibit q^{-D} behavior except in the case of $D=3$, where the behavior is related to the first derivative of $f(r)$ at $r = 0$.

The power-law pair-correlation function appears to be very useful in describing the fractal dimension and the shape and size of the clusters. It even seems plausible that by the choice of $f(r) = (1 - r/a)^\mu$ that fractal clusters of different types yet having the same fractal dimension might be distinguished from each other, as evidenced in the case of DLA and the DBM clusters of low dimensionality, as well as the Eden and ballistic cluster examples. The choice of $f(r) = (1 - r/a)^{D-1}$ was found to provide very suitable results for most of the clusters we examined. This suggests that the use of the shape parameter μ may not be necessary unless $f(r)$ can be shown to have different forms for clusters having the same value of D , but differing in their long-range structure. But it is intriguing that this term has the same type of dimensional scaling found at short range and works well for most of the fractals studied except DLA and the random polymer model. There is no analytical theory at this time that gives this interesting dimensional scaling.

We make the following observations about the correlation functions. The simple exponential function gives the worst estimate for the shape of the correlation function and thus very poor size results. The Gaussian function has a better shape, but cannot yield the fine structure in the fractal region or ever reproduce Porod (q^{-4}) scattering. These two models never give any oscillatory fine structure due to the absence of a size cutoff. The result of this is that these models give bad size information for clusters where $D=3$, because the fitting program will sacrifice accuracy in the Guinier region in an attempt to provide a better fit to the Porod region. Power-law functions always fit the Guinier region much better than the exponential function. Only the power-law functions can produce oscillatory scattering, and only the Gaussian model is at all comparable to the power-law models in being able to fit the proper R_g for the clusters. The conclusion is that the long-range order of the pair-correlation function for fractal clusters has a much sharper cutoff than is described by an exponential function. Since the exponential function is the cutoff function most frequently cited by authors in this field, it is important to be aware of its shortcomings.

Our research indicates that the simple power-law dependence of the q^{-D} type is only found for very large clusters or when the fractal dimension of the cluster is

very near $D=2$. Otherwise, a mild or pronounced oscillation is often superimposed on the q^{-D} scattering. This phenomenon is experimentally apparent when analyzing small monodisperse clusters such as silica spheres (Ludox).^{21,7} We demonstrate that this mild oscillatory effect can prevent the accurate determination of the fractal dimension as well as the size of the cluster when using scattering-intensity models based upon exponential pair-correlation functions as applied to any dilute and monodisperse systems. We have also found that the slopes of $\ln I(q)$ vs $\ln q$ in the fractal region are often not fit well when using the exponential model. Sometimes this appears to affect the D value and sometimes it does not. There appears to be the smallest influence on D when it is very near $D = 3$, and this is consistent with the discussion in the next paragraph.

Previous work has found special interest in a scattering intensity that is proportional to $q^{-\nu}$ where $3 \leq \nu < 4$, and we wish to address this case from the perspective of our models for mass fractals. This scattering case is ascribed to the presence of surface fractals as has been done in the important work of Bale and Schmidt.^{46,23} Their theory describes scattering from a surface fractal by the relation $\nu = D_s - 6$. D_s is the fractal dimension of the surface, which can have a value in the range $2 \leq D_s \leq 3$. The object is also assumed to have a constant density $D = 3$. This surface fractal theory is used to account for scattering with an exponent ν between 3 and 4. In our theory, there is no explicit division between bulk and surface atoms. We only consider the pair-correlation function $p(r)$, which will contain contributions from interior and "surface" atoms. In particular, the D that we calculate simply gives small- r dependence of $p(r)$. For $D = 3$ mass scaling the small- r dependence will be proportional to r^2 for a large cluster, but the presence of a rough surface can modify this scaling for smaller clusters. The scaling will be determined by an effective value of D , which will be slightly less than 3. This will give scattering that will have an effective ν between 3 and 4. By way of example the modified power correlation function predicts that the nonoscillatory scattering for $D = 3 - \delta$ with δ small will be

$$A f_p = \Gamma(2 - \delta) \left(\frac{\sin(\frac{\pi\delta}{2})}{q^{3-\delta}} + \frac{(2 - \delta)^2}{a q^{4-\delta}} + \dots \right). \quad (50)$$

As δ is increased from 0, the scattering exponent will decrease from 4. However, we note that our mass-fractal theory can never produce $I(q)$ that varies strictly as $q^{-\nu}$ with ν between 3 and 4. The relative sizes of the q^{-D} and $q^{-(D+1)}$ terms will depend on the precise form of $f(r)$ in addition to the fractal dimension and size of the cluster, but the effect will be the same. For a given size cluster, q^{-D} scattering dependence will be found for D sufficiently less than 3.

The recent work of Schmidt *et al.*¹¹ on scattering with exponents which exceed the Porod value of 4 is also relevant for the present work. Such scattering is found for reversed-phase (RP) silicas. Our assumed forms for $p(r)$ are not able to explain the results obtained for these systems. However, we have found scattering with exponents

greater than 4 for Debye scattering by geometric objects with two decidedly different physical dimensions. Examples include arrays of atoms that look like long tubes or boards.

Our global fits for $I(q)$ produce the best values of D that are consistent with the assumed form of $p(r)$. This D is seen to agree with other estimates of D for the clusters¹³ when the assumed $p(r)$ fits the scattering over the entire range of q . However, the exponential model does not provide good global fits, and its D parameter is greater than 3.1 for Eden clusters and spheres. Such non-physical values arise from the fact that the exponential $p(r)$ is a poor representation of the actual pair-correlation function for compact clusters.

The power models appear to have at least two interesting trends that suggest they are better than the Gaussian or exponential models in determinations of the fractal dimension D . The most important trend of the power models is their ability to accurately define D for compact clusters, where there are very small differences in the fractal dimension value for compact structures and near-compact structures such as the DBM $\eta=0.25$ cluster. Since the exponential model generally overestimates the value of D for most clusters, it is not an appropriate model for discerning the value of D for near-compact clusters. The Gaussian is also not appropriate for examining compact clusters for exactly the opposite reason that it generally underestimates the value of D for most clusters. For clusters of lower dimensionality where $D \leq 2$, the power and Gaussian models are much better than the exponential model in giving agreement with literature and mean-field fractal dimension values. The exponential model appears to only reproduce the D value of DLA, where the value agrees with mean-field theory.

The above discussion indicates that the power correlation functions give the best fractal dimensions. However, our results are based on fits to a single cluster and we have not averaged our results with data from many random clusters of the same type and size. Also we have not systematically determined the fractal dimensions of our clusters with an independent method such as R_g or $p(r)$ analysis, since we feel there are many ambiguities in these methods (such as different results in different ranges of N or r). In any case the values of D rendered by the power models for DLA clusters are well within any accepted boundaries, and the improved χ^2 of the power models over the exponential model more than justifies its use. The Gaussian model provides a slight enigma in the case of DLA. Since the Gaussian model has the best values of χ^2 for all of the DLA clusters, it would be expected that the D values it fits and the R_g values it produces should be very good. But instead the Gaussian model fits very poor values of R_g and produces very suspect values of D for a DLA cluster.

The second trend can be observed in the DBM clusters. The power models yield values of D for the lower values of η that are slightly high with respect to the mean-field-theory values. However, as η is increased the χ^2 of the fits decreases and the values of D approach the predicted mean-field values. The most important reason for this behavior appears to be that the oscillations are

being damped by the lower values of D and the increasing spanning length. The Gaussian model by comparison always produces lower D values than predicted by mean-field theory with the maximum discrepancy found when $\eta=1.0$. This is opposite to the behavior of the power models. The exponential model produces values of D which are consistently much higher than those predicted by mean-field theory. This argues against there being some statistical aberration for our single examples of clusters since the deviations of D from the mean-field values are consistent for different values for η . Although the fractal dimensions obtained from the exponential model agree better with experimental data,¹⁹ this result may be partly due the fact that our DBM clusters are much larger than those used in the experiment. The method used to determine D can also significantly affect the value. A significant conclusion should be drawn that the properties of $f(r)$ directly affect the fractal measure found for any cluster examined. To conclusively prove that the power models are producing the best results in all the cases would require work beyond the scope of this paper. We do, however, feel that in all cases the power models produce results which are very close or exactly in agreement with experimental and or theoretical values of the fractal dimension. The power models never produce contradictory or suspect results such as those found in the Gaussian or exponential model, especially the exponential model. The one or two cases where the results from the exponential or Gaussian model appear to be slightly better or equivalent to the power models is far outweighed by inferior χ^2 values and poor R_g values produced by those models.

When fitting Debye scattering data with power correlation functions, we find fitted spanning lengths that are between 60% and 90% of the real spanning lengths for the cluster (see Table VI). We also find oscillations in the fitted scattering intensity that do not damp out with increasing q as is found in the Debye data. These two observations are related to the fact that the actual pair-correlation function for the random clusters has a very long but small-amplitude tail. This tail is seen in Figs. 7–12 as the part of the actual correlation function with “zero” amplitude to $r/a = 1$. The actual cluster by its random nature has a small measure set of distances that are significantly greater than those needed to produce the main features of the scattering. The tail of the real correlation function is not contained in our analytic correlation function, and it has an extremely small integrated area. However, this small part of the correlation function is capable of damping out the oscillations in $I(q)$. Figure 13 has two curves that represent Debye-sum data for a 100 000-particle ballistic cluster. The curve without large- q oscillations is the result of transforming all pair distances in the cluster. The other curve is the result of transforming 99.9% of the total pair distances. The two $I(q)$ curves are coincident for $q < 0.2$. Clear oscillatory behavior at large q is evident for the second curve. This oscillatory nature is very similar to what we observe for fitting several of the clusters. The actual cluster coordinates will have oscillatory scattering if the fuzzy surface of the cluster is shaved off. However, the slope of $I(q)$ is

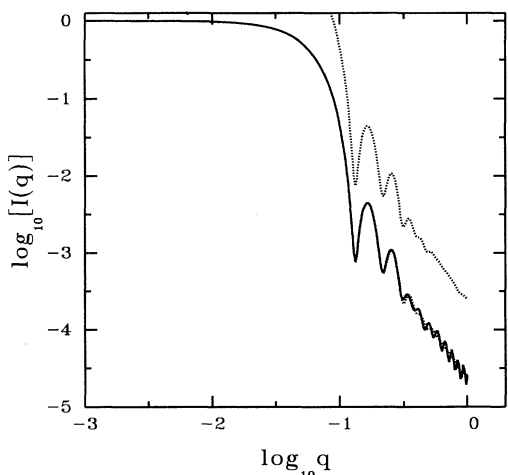


FIG. 13. Effect of the tail in a ballistic random cluster on $I(q)$. The solid line is the Debye sum for all pair distances. The dotted line (displaced up by $1 \log_{10}$ unit) omits the largest 0.1% of the pair distances. The dotted line is also shown without displacement, where it is seen to be indistinguishable from the solid line for $\log_{10} < -0.7$.

not affected by the elimination of the tail. The oscillations in $I(q)$ are damped by including only 0.1% of the total pair distances. For this 100 000-particle cluster, this could represent the pair distances of only 100 particles. The last 0.1% of the total pair distances are associated with $r/a \geq 0.82$. This distance is consistent with the spanning length fit by the three-parameter power model (see Table VI). Similar truncation results are found for the other compact random clusters, but the effect is not observable for DLA and the more fractal DBM clusters.

The small-angle scattering is very sensitive to the form of $f(r)$ for compact clusters. For these clusters the parameter μ in the three-parameter power fits is often given as $D - 1$. The cases where $\mu \neq D - 1$ appear to indicate differences in the correlation functions that may be caused by angular or radial anisotropy or by the presence of multiple mass scaling terms. However, there is ample evidence in this work that the scattering for $D = 2$ objects is insensitive to the form of $f(r)$. The data for Eden clusters grown on a plane and the TSAW polymer grown in 3D space and the above analysis support this conclusion.

The power pair-correlation functions provide a good fit to the Debye scattering and the actual correlation functions for most of the clusters in this work. However, the fits to DLA clusters are less satisfactory. The anisotropies stated above might give the DLA clusters a $p(r)$ that cannot be approximated by our assumed forms. Another explanation is that the multifractal nature of DLA is expressed in the small-angle scattering. For a multifractal we expect the mass to scale with an expression such as

$$p(r) = \sum_i \alpha_i r^{D_i-1} f_i(r), \quad (51)$$

where α_i is the amplitude of the component that scales as D_i . The $f_i(r)$ can have the same or different size given by a parameter such as a_i .

The scattering exponent will be affected if two or more terms with sufficiently different D_i have significant amplitudes. If the size parameters a_i are similar, then the scattering exponent will be determined by the smaller value of D_i . The effect will be seen because the scattering intensity falls off less rapidly for small values of the fractal dimension. If the size parameters are very different, then the scattering exponent may have one value in one q range and another in a different q range. This can be seen in the Debye-sum scattering for scatterers placed at the positions (i, j) where $1 \leq i \leq 50$ and $1 \leq j \leq 2$. In this case $\nu = 1$ for $0.1 < q < 1$ and $\nu = 2$ for $2 < q < 4$. Finally, it appears that the D value obtained from analysis of the scattering by a multifractal can be different than the D given by R_g or $p(r)$ analysis. If several terms in Eq. (51) have significant values for α , expressing $p(r)$ with Eq. (1) may introduce considerable error. The scattering intensity $I(q)$ is easily obtained for $p(r)$ given by Eq. (51), but we do not use Eq. (51) in this work because the number of adjustable parameters can easily get out of control.

ACKNOWLEDGMENTS

We wish to thank the National Science Foundation for supercomputer time at Illinois and San Diego under Grant No. CHE900022N. We also thank Dr. Paul Meakin for sending us the coordinates of the 10 000-atom off-lattice DLA cluster and Troy Wahl for deriving Eq. (21).

¹ P. Meakin, in *Phase Transitions and Critical Phenomena*, edited by C. Domb and J. L. Lebowitz (Academic, New York, 1987), Vol. 12.

² P. Meakin, *Phys. Rev. A* **27**, 1495 (1983).

³ T. A. Witten and L. M. Sander, *Phys. Rev. Lett.* **47**, 1400 (1981).

⁴ A. Guinier and G. Fournet, *Small-Angle Scattering of X-Rays* (Wiley, New York, 1955).

⁵ T. A. Witten and L. M. Sander, *Phys. Rev. B* **27**, 5686 (1983).

⁶ D. W. Schaefer, J. E. Martin, P. Wiltzius, and D. S. Cannel,

Phys. Rev. Lett. **52**, 2371 (1984).

⁷ M. Foret, J. Pelous, and R. Vacher, *J. Phys. (Paris) I* **2**, 791 (1992).

⁸ C. Chachaty, J. P. Korb, J. R. C. van der Maarel, W. Bras, and P. Quinn, *Phys. Rev. B* **44**, 4778 (1991).

⁹ R. Giordano, A. Grasso, J. Teixeira, and U. Wanderlingh, *Physica B* **180**, 762 (1992).

¹⁰ X. H. Guo, N. M. Zhao, S. H. Chen, and J. Teixeira, *Biopolymers* **29**, 335 (1990).

¹¹ P. W. Schmidt, A. Höhr, M. Steiner, and A. Röhl, *J. Chem. Phys.* **94**, 1474 (1991).

- ¹² S. Nemmers, D. K. Horne, and H. D. Bale, *J. Appl. Phys.* **68**, 3178 (1990).
- ¹³ T. Vicsek, *Fractal Growth Phenomena* (World Scientific, Singapore, 1989).
- ¹⁴ P. Meakin and T. Vicsek, *Phys. Rev. A* **32**, 685 (1985).
- ¹⁵ M. Eden (unpublished).
- ¹⁶ P. Meakin, *J. Colloid Interface Sci.* **105**, 240 (1985).
- ¹⁷ L. Niemeyer, L. Pietronero, and H. J. Wiesmann, *Phys. Rev. Lett.* **52**, 1033 (1984).
- ¹⁸ L. Pietronero, A. Erzan, and C. Evertsz, *Phys. Rev. Lett.* **61**, 861 (1988).
- ¹⁹ H. J. Wiesmann and L. Pietronero, in *Fractals in Physics*, edited by L. Pietronero and E. Tossati (North-Holland, Amsterdam, 1986).
- ²⁰ B. A. Fedorov and P. W. Schmidt, *Biofizika* **36**, 749 (1991).
- ²¹ W. S. Rothwell, *J. Appl. Phys.* **39**, 1840 (1967).
- ²² J. Teixeira, in *On Growth and Form*, edited by H. E. Stanley and N. Ostrowsky (Nijhoff, Dordrecht, 1986).
- ²³ P. W. Schmidt, *J. Appl. Crystallogr.* **24**, 414 (1991).
- ²⁴ S. K. Sinha, *Physica D* **38**, 310 (1989).
- ²⁵ *Handbook of Mathematical Functions*, edited by M. Abramowitz and I. A. Stegun, Natl. Bur. Stand. Appl. Math. Ser. No. 55 (U.S. GPO, Washington, D.C., 1965).
- ²⁶ P. Mangin, B. Rodmacq, and A. Chamberod, *Phys. Rev. Lett.* **55**, 2899 (1985).
- ²⁷ J. Teixeira, *J. Appl. Cryst.* **21**, 781 (1988).
- ²⁸ J. Teixeira, *New J. Chem.* **14**, 217 (1990).
- ²⁹ *Tables of Integral Transforms*, edited by A. Erdélyi (McGraw-Hill, New York, 1954).
- ³⁰ I. S. Gradshteyn and I. M. Ryzhik, *Table of Integrals, Series, and Products* (Academic, New York, 1980).
- ³¹ Y. L. Luke, *Algorithms for the Computation of Mathematical Functions* (Academic, New York, 1977).
- ³² R. C. Ball and T. A. Witten, *Phys. Rev. A* **29**, 2966 (1984).
- ³³ S. Tolman and P. Meakin, *Physica A* **158**, 801 (1989).
- ³⁴ M. Matsuhita, K. Honda, H. Toyoki, Y. Hayakawa, and H. Kondo, *J. Phys. Soc. Jpn.* **55**, 2618 (1986).
- ³⁵ L. Pietronero, *Physica D* **38**, 279 (1989).
- ³⁶ M. Marsili and L. Pietronero, *Physica A* **175**, 31 (1991).
- ³⁷ C. Evertsz, *Phys. Rev. A* **32**, 1830 (1990).
- ³⁸ J. H. Kaufman, G. M. Dimino, and P. Meakin, *Physica A* **157**, 656 (1989).
- ³⁹ L. A. Turkevich and H. Scher, *Phys. Rev. Lett.* **55**, 1026 (1985).
- ⁴⁰ R. C. Ball, R. M. Brady, G. Rossi, and B. R. Thompson, *Phys. Rev. Lett.* **55**, 1406 (1985).
- ⁴¹ M. Plischke and Z. Răcz, *Phys. Rev. Lett.* **53**, 415 (1984).
- ⁴² A. Vespignani and L. Pietronero, *Physica A* **173**, 1 (1991).
- ⁴³ S. P. Obukhov and L. Peliti, *J. Phys. A* **33**, L147 (1983).
- ⁴⁴ P. Debye, *J. Phys. Colloid Chem.* **51**, 18 (1947).
- ⁴⁵ S. Liang and L. P. Kadanoff, *Phys. Rev. A* **31**, 2628 (1985).
- ⁴⁶ H. D. Bale and P. W. Schmidt, *Phys. Rev. Lett.* **53**, 596 (1984).